

ful to Kyowa Hakko Kirin for providing TPO and G-CSF. We also thank the Center for Anatomical Studies, Kyoto University Graduate School of Medicine, for immunocytochemical analysis. Funding was provided by grants from the Ministry of Health, Labour and Welfare to KW, TN, and TH, a grant from the Ministry of Education, Culture, Sports, Science and Technology (MEXT) to KW, TN, and TH, grants from the Leading Project of MEXT to TN, a grant from Funding Program for World-Leading Innovative Research and Development on Science and Technology (FIRST Program) of Japan Society for the Promotion

of Science (JSPS) to TN, grants from the SENSHIN Medical Research Foundation to IK, and grants from the Fujiwara Memorial Foundation to TM. This work was also supported by the Global COE Program "Center for Frontier Medicine" from MEXT, Japan.

Authorship and Disclosures

Information on authorship, contributions, and financial & other disclosures was provided by the authors and is available with the online version of this article at www.haematologica.org.

References

- Welte K, Zeidler C, Dale DC. Severe congenital neutropenia. *Semin Hematol*. 2006;43(3):189-95.
- Skokowa J, Germeshausen M, Zeidler C, Welte K. Severe congenital neutropenia: inheritance and pathophysiology. *Curr Opin Hematol*. 2007;14(1):22-8.
- Dale DC, Person RE, Bolyard AA, Aprikyan AG, Bos C, Bonilla MA, et al. Mutations in the gene encoding neutrophil elastase in congenital and cyclic neutropenia. *Blood*. 2000;96(7):2317-22.
- Kostmann R. Infantile genetic agranulocytosis; agranulocytosis infantilis hereditaria. *Acta Paediatr Suppl*. 1956;45(Suppl 105):1-78.
- Klein C, Grudzien M, Appaswamy G, Germeshausen M, Sandrock I, Schaffer AA, et al. HAX1 deficiency causes autosomal recessive severe congenital neutropenia (Kostmann disease). *Nat Genet*. 2007;39(1):86-92.
- Suzuki Y, Demoliere C, Kitamura D, Takeshita H, Deuschle U, Watanabe T. HAX-1, a novel intracellular protein, localized on mitochondria, directly associates with HS1, a substrate of Src family tyrosine kinases. *J Immunol*. 1997;158(6):2736-44.
- Sharp TV, Wang HW, Koumi A, Hollyman D, Endo Y, Ye H, et al. K15 protein of Kaposi's sarcoma-associated herpesvirus is latently expressed and binds to HAX-1, a protein with antiapoptotic function. *J Virol*. 2002;76(2):802-16.
- Freedman MH, Bonilla MA, Fier C, Bolyard AA, Scarlata D, Boxer LA, et al. Myelodysplasia syndrome and acute myeloid leukemia in patients with congenital neutropenia receiving G-CSF therapy. *Blood*. 2000;96(2):429-36.
- Rosenberg PS, Zeidler C, Bolyard AA, Alter BP, Bonilla MA, Boxer LA, et al. Stable long-term risk of leukaemia in patients with severe congenital neutropenia maintained on G-CSF therapy. *Br J Haematol*. 2010;150(2):196-9.
- Chao JR, Parganas E, Boyd K, Hong CY, Opferman JT, Ihle JN. Hax1-mediated processing of HtrA2 by Parl allows survival of lymphocytes and neurons. *Nature*. 2008;452(7183):98-102.
- Takahashi K, Yamanaka S. Induction of pluripotent stem cells from mouse embryonic and adult fibroblast cultures by defined factors. *Cell*. 2006;126(4):663-76.
- Takahashi K, Tanabe K, Ohnuki M, Narita M, Ichisaka T, Tomoda K, et al. Induction of pluripotent stem cells from adult human fibroblasts by defined factors. *Cell*. 2007;131(5):861-72.
- Meissner A, Wernig M, Jaenisch R. Direct reprogramming of genetically unmodified fibroblasts into pluripotent stem cells. *Nat Biotechnol*. 2007;25(10):1177-81.
- Okita K, Ichisaka T, Yamanaka S. Generation of germline-competent induced pluripotent stem cells. *Nature*. 2007;448(7151):313-7.
- Park IH, Zhao R, West JA, Yabuuchi A, Huo H, Ince TA, et al. Reprogramming of human somatic cells to pluripotency with defined factors. *Nature*. 2008;451(7175):141-6.
- Yu J, Vodyanik MA, Smuga-Otto K, Antosiewicz-Bourget J, Frane JM, Tian S, et al. Induced pluripotent stem cell lines derived from human somatic cells. *Science*. 2007;318(5858):1917-20.
- Morishima T, Watanabe K, Niwa A, Fujino H, Matsubara H, Adachi S, et al. Neutrophil differentiation from human-induced pluripotent stem cells. *J Cell Physiol*. 2011;226(5):1283-91.
- Niwa A, Heike T, Umeda K, Oshima K, Kato I, Sakai H, et al. A novel serum-free monolayer culture for orderly hematopoietic differentiation of human pluripotent cells via mesodermal progenitors. *PLoS One*. 2011;6(7):e22261.
- Matsubara K, Imai K, Okada S, Miki M, Ishikawa N, Tsumura M, et al. Severe developmental delay and epilepsy in a Japanese patient with severe congenital neutropenia due to HAX1 deficiency. *Haematologica*. 2007;92(12):e123-5.
- Skokowa J, Fobiwe JP, Dan L, Thakur BK, Welte K. Neutrophil elastase is severely down-regulated in severe congenital neutropenia independent of ELA2 or HAX1 mutations but dependent on LEF-1. *Blood*. 2009;114(14):3044-51.
- Kobayashi M, Yumiba C, Kawaguchi Y, Tanaka Y, Ueda K, Komazawa Y, et al. Abnormal responses of myeloid progenitor cells to recombinant human colony-stimulating factors in congenital neutropenia. *Blood*. 1990;75(11):2143-9.
- Konishi N, Kobayashi M, Miyagawa S, Sato T, Katoh O, Ueda K. Defective proliferation of primitive myeloid progenitor cells in patients with severe congenital neutropenia. *Blood*. 1999;94(12):4077-83.
- Germeshausen M, Grudzien M, Zeidler C, Abdollahpour H, Yergin S, Rezaei N, et al. Novel HAX1 mutations in patients with severe congenital neutropenia reveal isoform-dependent genotype-phenotype associations. *Blood*. 2008;111(10):4954-7.
- Hiramoto T, Ebihara Y, Mizoguchi Y, Nakamura K, Yamaguchi K, Ueno K, et al. Wnt3a stimulates maturation of impaired neutrophils developed from severe congenital neutropenia patient-derived pluripotent stem cells. *Proc Natl Acad Sci USA*. 2013;110(8):3023-8.
- Hacein-Bey-Abina S, Von Kalle C, Schmidt M, McCormack MP, Wulffraat N, Leboulch P, et al. LMO2-associated clonal T cell proliferation in two patients after gene therapy for SCID-X1. *Science*. 2003;302(5644):415-9.
- Ott MG, Schmidt M, Schwarzwaelder K, Stein S, Siler U, Koehl U, et al. Correction of X-linked chronic granulomatous disease by gene therapy, augmented by insertional activation of MDS1-EV11, PRDM16 or SETBP1. *Nat Med*. 2006;12(4):401-9.
- Howe SJ, Mansour MR, Schwarzwaelder K, Bartholomae C, Hubank M, Kempinski H, et al. Insertional mutagenesis combined with acquired somatic mutations causes leukemogenesis following gene therapy of SCID-X1 patients. *J Clin Invest*. 2008;118(9):3143-50.
- Cavazzana-Calvo M, Payen E, Negre O, Wang G, Hehir K, Fusil F, et al. Transfusion independence and HMGA2 activation after gene therapy of human beta-thalassaemia. *Nature*. 2010;467(7313):318-22.
- Papapetrou EP, Lee G, Malani N, Setty M, Riviere I, Tirunagari LM, et al. Genomic safe harbors permit high beta-globin transgene expression in thalassemia induced pluripotent stem cells. *Nat Biotechnol*. 2011;29(1):73-8.
- Zou J, Sweeney CL, Chou BK, Choi U, Pan J, Wang H, et al. Oxidase-deficient neutrophils from X-linked chronic granulomatous disease iPSCs: functional correction by zinc finger nuclease-mediated safe harbor targeting. *Blood*. 2011;117(21):5561-72.
- DeKelver RC, Choi VM, Moehle EA, Paschon DE, Hockemeyer D, Meisinger SH, et al. Functional genomics, proteomics, and regulatory DNA analysis in isogenic settings using zinc finger nuclease-driven transgenesis into a safe harbor locus in the human genome. *Genome Res*. 2010;20(8):1133-42.
- Hockemeyer D, Soldner F, Beard C, Gao Q, Mitalipova M, DeKelver RC, et al. Efficient targeting of expressed and silent genes in human ESCs and iPSCs using zinc-finger nucleases. *Nat Biotechnol*. 2009;27(9):851-7.
- Henckaerts E, Dutheil N, Zeltner N, Kattman S, Kohlbrenner E, Ward P, et al. Site-specific integration of adeno-associated virus involves partial duplication of the target locus. *Proc Natl Acad Sci USA*. 2009;106(18):7571-6.
- Ishikawa N, Okada S, Miki M, Shirao K, Kihara H, Tsumura M, et al. Neurodevelopmental abnormalities associated with severe congenital neutropenia due to the R86X mutation in the HAX1 gene. *J Med Genet*. 2008;45(12):802-7.

Robust and Highly-Efficient Differentiation of Functional Monocytic Cells from Human Pluripotent Stem Cells under Serum- and Feeder Cell-Free Conditions

Masakatsu D. Yanagimachi^{1,4}, Akira Niwa¹, Takayuki Tanaka¹, Fumiko Honda-Ozaki¹, Seiko Nishimoto¹, Yuuki Murata³, Takahiro Yasumi³, Jun Ito¹, Shota Tomida¹, Koichi Oshima¹, Isao Asaka², Hiroaki Goto⁴, Toshio Heike³, Tatsutoshi Nakahata¹, Megumu K. Saito^{1*}

¹ Department of Clinical Application, Center for iPS Cell Research and Application, Kyoto University, Kyoto, Japan, ² Department of Fundamental Cell Technology, Center for iPS Cell Research and Application, Kyoto University, Kyoto, Japan, ³ Department of Pediatrics, Kyoto University Graduate School of Medicine, Kyoto, Japan, ⁴ Department of Pediatrics, Yokohama City University Graduate School of Medicine, Yokohama, Japan

Abstract

Monocytic lineage cells (monocytes, macrophages and dendritic cells) play important roles in immune responses and are involved in various pathological conditions. The development of monocytic cells from human embryonic stem cells (ESCs) and induced pluripotent stem cells (iPSCs) is of particular interest because it provides an unlimited cell source for clinical application and basic research on disease pathology. Although the methods for monocytic cell differentiation from ESCs/iPSCs using embryonic body or feeder co-culture systems have already been established, these methods depend on the use of xenogeneic materials and, therefore, have a relatively poor-reproducibility. Here, we established a robust and highly-efficient method to differentiate functional monocytic cells from ESCs/iPSCs under serum- and feeder cell-free conditions. This method produced $1.3 \times 10^6 \pm 0.3 \times 10^6$ floating monocytes from approximately 30 clusters of ESCs/iPSCs 5–6 times per course of differentiation. Such monocytes could be differentiated into functional macrophages and dendritic cells. This method should be useful for regenerative medicine, disease-specific iPSC studies and drug discovery.

Citation: Yanagimachi MD, Niwa A, Tanaka T, Honda-Ozaki F, Nishimoto S, et al. (2013) Robust and Highly-Efficient Differentiation of Functional Monocytic Cells from Human Pluripotent Stem Cells under Serum- and Feeder Cell-Free Conditions. PLoS ONE 8(4): e59243. doi:10.1371/journal.pone.0059243

Editor: Katriina Aalto-Setälä, University of Tampere, Finland

Received: August 14, 2012; **Accepted:** February 13, 2013; **Published:** April 3, 2013

Copyright: © 2013 Yanagimachi et al. This is an open-access article distributed under the terms of the Creative Commons Attribution License, which permits unrestricted use, distribution, and reproduction in any medium, provided the original author and source are credited.

Funding: Funding was provided by grants from the Ministry of Health, Labour and Welfare to TN, a grant from the Ministry of Education, Culture, Sports, Science and Technology (MEXT) to TN, grants from the Leading Project of MEXT to TN, a grant from Funding Program for World-Leading Innovative Research and Development on Science and Technology (FIRST Program) of Japan Society for the Promotion of Science (JSPS) to TN, grants from JSPS to TN and MKS, grants from the Takeda foundation, Mitsubishi Pharma Research Foundation and Suzuken memorial foundation to MKS and grants from Grants-in-Aid for Scientific Research from Japan Society for the Promotion of Science from the Ministry of Education, Culture, Sports, Science, and Technology of Japan to MDY. The funders had no role in study design, data collection and analysis, decision to publish, or preparation of the manuscript.

Competing Interests: The authors have declared that no competing interests exist.

* E-mail: msaito@cira.kyoto-u.ac.jp

Introduction

Monocytic lineage cells, such as monocytes, macrophages and dendritic cells (DCs), are central to immune responses and play key roles in various pathological conditions. [1–2] Monocytes are the myeloid progeny of hematopoietic stem/progenitor cells [3]; they are a type of mononuclear cell circulating in the bloodstream and act as gatekeepers in innate immunity. While they replenish macrophages and DCs, monocytes themselves respond to various inflammatory stimuli by migrating into inflamed tissues, phagocytosing pathological small particles and producing proinflammatory cytokines and chemokines. Therefore, monocytes not only contribute to host defense against pathogenic microorganisms, but are closely associated with the pathogenesis of chronic sterile inflammation. [4] Macrophages reside in tissues and robustly phagocytose microorganisms and cellular debris. One of the important hallmarks of monocytic lineage cells is their functional plasticity. In response to cytokines and microbial products, macrophages polarize into functionally distinct M1 and M2 cells. [5] Classically activated M1 macrophages are induced by interferon- γ (IFN γ), while alternatively activated M2 macrophages

can be induced by IL-4 and IL-13. [2,5] M1 macrophages are generally characterized by high production of proinflammatory cytokines, while M2 are characterized by high production of anti-inflammatory cytokines. DCs are the most powerful antigen-presenting cells and have an indispensable role for the activation of T lymphocytes. Because of their ability to mediate communication between innate and acquired immunity, ex vivo expansion of DCs is expected to be a useful source of material for cancer immunotherapies, such as DC-based vaccines. [6–7] Moreover, recent reports of monocyte and/or DC deficiencies highlight the importance of understanding their development in humans. [8] However, there have been technical limitations for tracing the development of human monocytic cells, or for propagating them ex vivo.

Human embryonic stem cells (ESCs) and induced pluripotent stem cells (iPSCs) are undifferentiated pluripotent cells that can be propagated indefinitely. [9–11] The development of monocytic cells from these pluripotent cells is of particular interest because it would provide an unlimited source of these cells for clinical applications and the examination of disease pathologies. Although the methods for hematopoietic differentiation from ESCs/iPSCs

using embryonic body or feeder co-culture systems have already been established, [12] these methods usually depend on xenogeneic feeder cells and/or animal- or human-derived serum, and therefore have a relatively poor-reproducibility. For instance, batch-to-batch variability of serum or feeder cells can influence the characteristics of *in vitro* differentiated DCs. [13] Here, we describe a novel serum- and feeder cell-free method that robustly and repetitively produces monocytic lineage cells from human ESCs/iPSCs.

Materials and Methods

Cell Culture

This study used human ESCs (cell line: KhES1) and iPSCs (cell lines: 201B7, 253G4, CIRA188Ai-W2, and CB-A11). [10,14–15] 201B7, 253G4 [10] and CIRA188Ai-W2 [15] were previously described. A human ES cell line KhES1 was kindly provided by Dr. Norio Nakatsuji. Human iPS cell lines 201B7 and 253G4 were kindly provided by Dr. Shinya Yamanaka. CB-A11 was established from cord-blood mononuclear cells by using episomal vectors. [16] These ESCs/iPSCs were maintained on tissue culture dishes coated with growth factor-reduced Matrigel (Becton-Dickinson) in mTeSR1 serum-free medium (STEMCELL Technologies).

Monocytic Lineage Cell Differentiation Method

The monocytic lineage differentiation protocol was modified from a previously established hematopoietic differentiation protocol (Figure 1). [17] The protocol consists of 5 sequential steps by which mature MPs and DCs are differentiated from human

pluripotent cells in a stepwise manner. In the first step, primitive streak cells were induced from undifferentiated ESCs/iPSCs, which were then differentiated into hemangioblast-like hematopoietic progenitors in the second step. In step 3, expanded hematopoietic progenitors were committed towards initial myeloid differentiation, and then differentiated into the monocytic lineage in step 4. Finally, CD14⁺ monocytes were differentiated into either MPs or DCs in step 5. The cytokines used in this study were purchased from R&D systems.

Step 1: induction of primitive streak-like cells from undifferentiated human ES/iPS cells with BMP4. BMP4 is an important molecule for the initial stage of mesodermal commitment of pluripotent stem cells *in vitro*. [17] Undifferentiated ESCs/iPSCs colonies were disseminated onto a 100 mm culture dish coated with growth factor-reduced Matrigel in mTeSR1 medium at a density of about 30 colonies per dish. Individual colonies were grown to a diameter of approximately 1 mm (Day 0), and BMP4 (80 ng/mL) was added to the mTeSR1 medium.

Step 2: generation of KDR⁺CD34⁺ hemangioblast-like cells with VEGF, basic FGF and SCF. VEGF and SCF have been reported to be important cytokines for development of hemoangiogenic progenitors. [18–19] In this step, we also added basic FGF which enhances the development of mesodermal hematopoietic progenitors. [18,20] The mTeSR1 medium was replaced by StemPro-34 serum-free medium (Gibco) containing 2 mM glutamax (Invitrogen) on day 4, and then was supplemented with the step-2 cytokine cocktail composed of VEGF (80 ng/mL), basic FGF (25 ng/mL), and SCF (100 ng/mL).

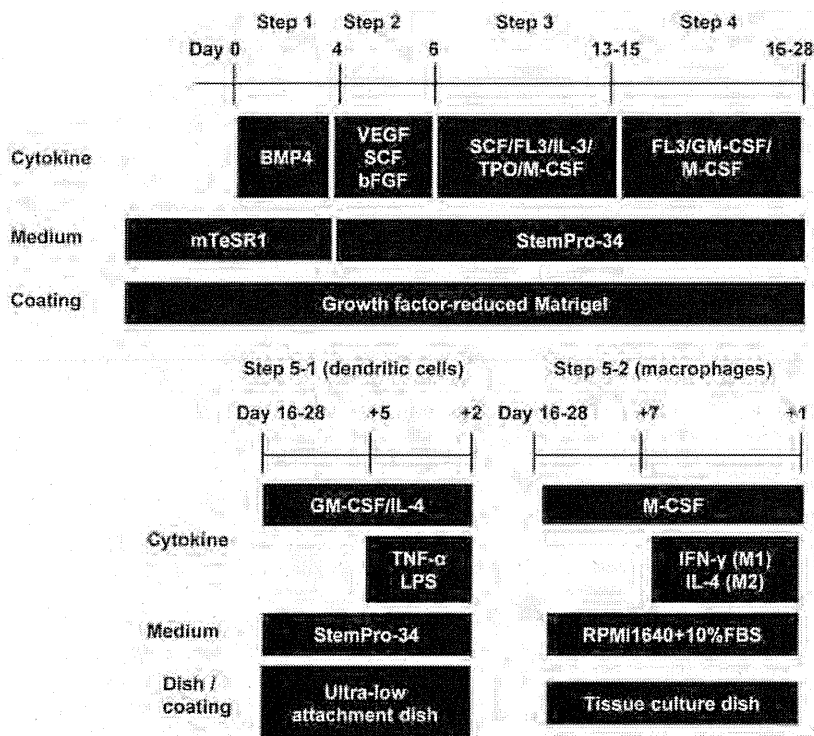


Figure 1. Protocol for monocytic lineage cell differentiation from human pluripotent stem cells. The protocol is composed of 5 steps. CD14-positive cells that are sorted between step-4 are differentiated into dendritic cells by step 5-1 or into macrophages by step 5-2. FL-3: Flt-3 ligand, TPO: Thrombopoietin.

doi:10.1371/journal.pone.0059243.g001

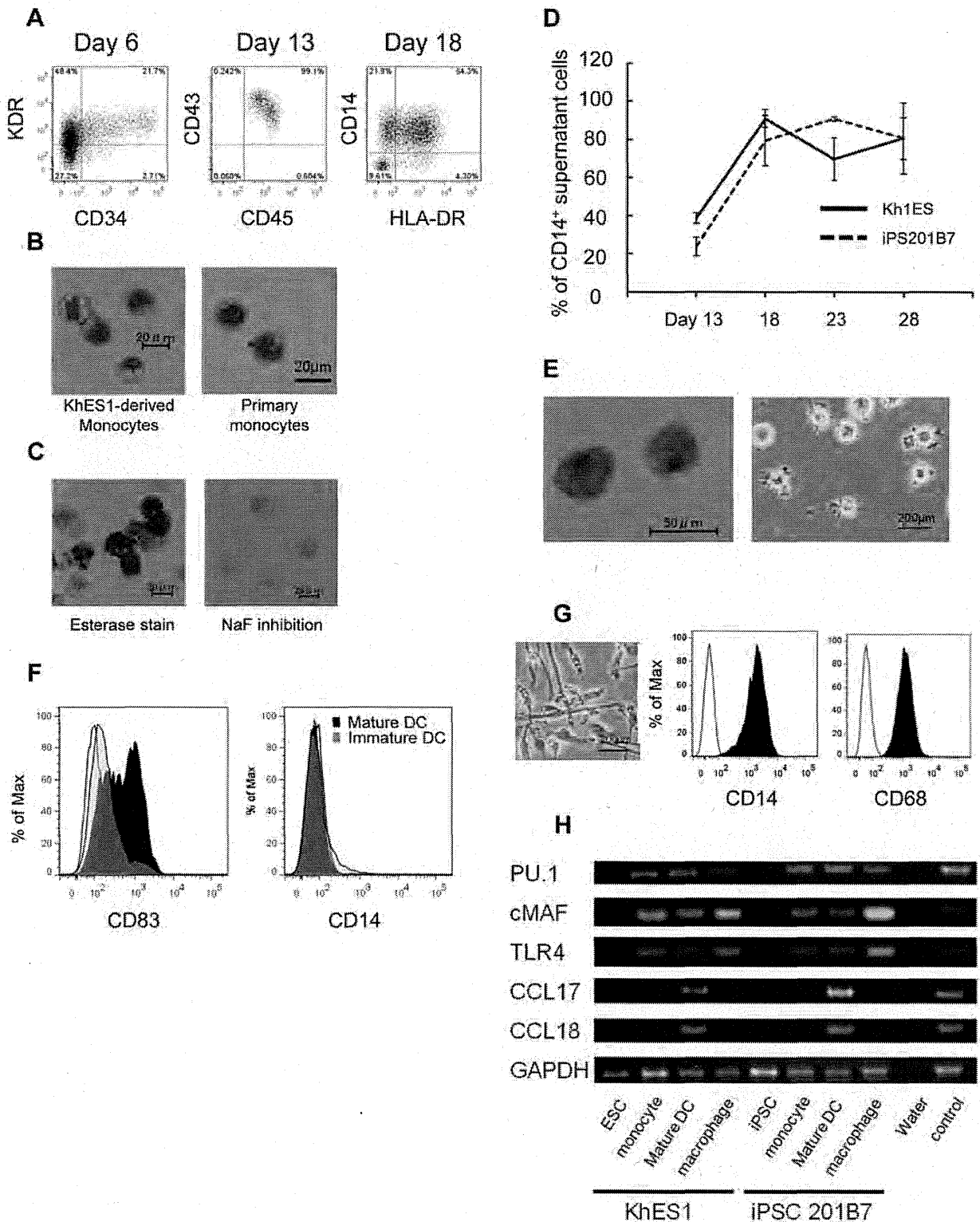


Figure 2. Phenotype analysis and gene expression pattern of monocytic lineage cells derived from pluripotent stem cells. (A) Flow cytometric analysis of monocytic lineage cells derived sequentially from pluripotent stem cells. An analysis of adherent cells on day 6 and supernatant cells on day 13 and 18 is shown. (B) May-Giemsa staining of CD14⁺ monocyte-like cells derived from KhES1 on day 16 (left) and primary human monocytes (right). (C) Esterase staining for CD14⁺ monocyte-like cells derived from KhES1 on day 16. (D) The percentage of CD14⁺ cells within the total floating cells derived from KhES1/iPSC-201B7 was evaluated from day 13 to day 28. (E) May-Giemsa staining (left) and phase contrast image (right)

of mature DCs derived from pluripotent stem cells. (F) Flow cytometric analysis of immature/mature DCs derived from pluripotent stem cells. (G) Phase contrast image and flow cytometric analysis of macrophages derived from pluripotent stem cells. (H) RT-PCR analysis of monocytic lineage cells derived from KhES1/iPS-201B7 clones for expression of monocytic lineage marker genes (*PU.1*, *c-MAF*, *TLR4*, *CCL17* and *CCL18*). Peripheral blood monocytes and peripheral blood monocyte-derived mature DCs were used as positive controls. (A–C, E–G) The data from KhES1-derived cells are shown as representative.

doi:10.1371/journal.pone.0059243.g002

Step 3: generation of hematopoietic cells with hematopoietic cytokines. The cytokines in StemPro-34 medium were switched to the step-3 cytokine cocktail composed of SCF (50 ng/mL), IL-3 (50 ng/mL), TPO (Thrombopoietin) (5 ng/mL), M-CSF (50 ng/mL), and Flt-3 ligand (50 ng/mL), on day 6. Thereafter, the medium was changed on day 10.

Step 4: monocytic lineage-directed differentiation with Flt-3 ligand, GM-CSF and M-CSF. The cytokines in StemPro-34 medium were switched to the step-4 cytokine cocktail composed of Flt-3 ligand (50 ng/mL), GM-CSF (25 ng/mL), and M-CSF (50 ng/mL) on day 13–15. The medium was changed every 3–4 days. The CD14⁺ monocytic lineage-directed cell fraction in supernatant was positively sorted by autoMACS pro

(Miltenyi Biotec) with CD14 MicroBeads (Miltenyi Biotec) on days 15–28.

Step 5: differentiation into DCs (step 5-1) and MPs (step 5-2) from CD14⁺ monocytic lineage-cells. CD14⁺ cells sorted by autoMACS pro (1.5×10^6 cells per well in a 6-well plate with Ultra-Low Attachment Surface (CORNING)) were cultured in StemPro-34 medium supplemented with GM-CSF (25 ng/mL) and IL-4 (40 ng/mL), with a medium change 4 days later, for differentiation into DCs (step 5-1). LPS (100 ng/mL, InvivoGen) and TNF α (0.2 ng/mL) were added for the last 2 days of the 7 day DC differentiation culture to promote maturation of DCs. CD14⁺ cells (1.5×10^6 cells per well in a 6-well tissue culture plate) were cultured in RPMI-1640 medium (Sigma) supplemented with 10%

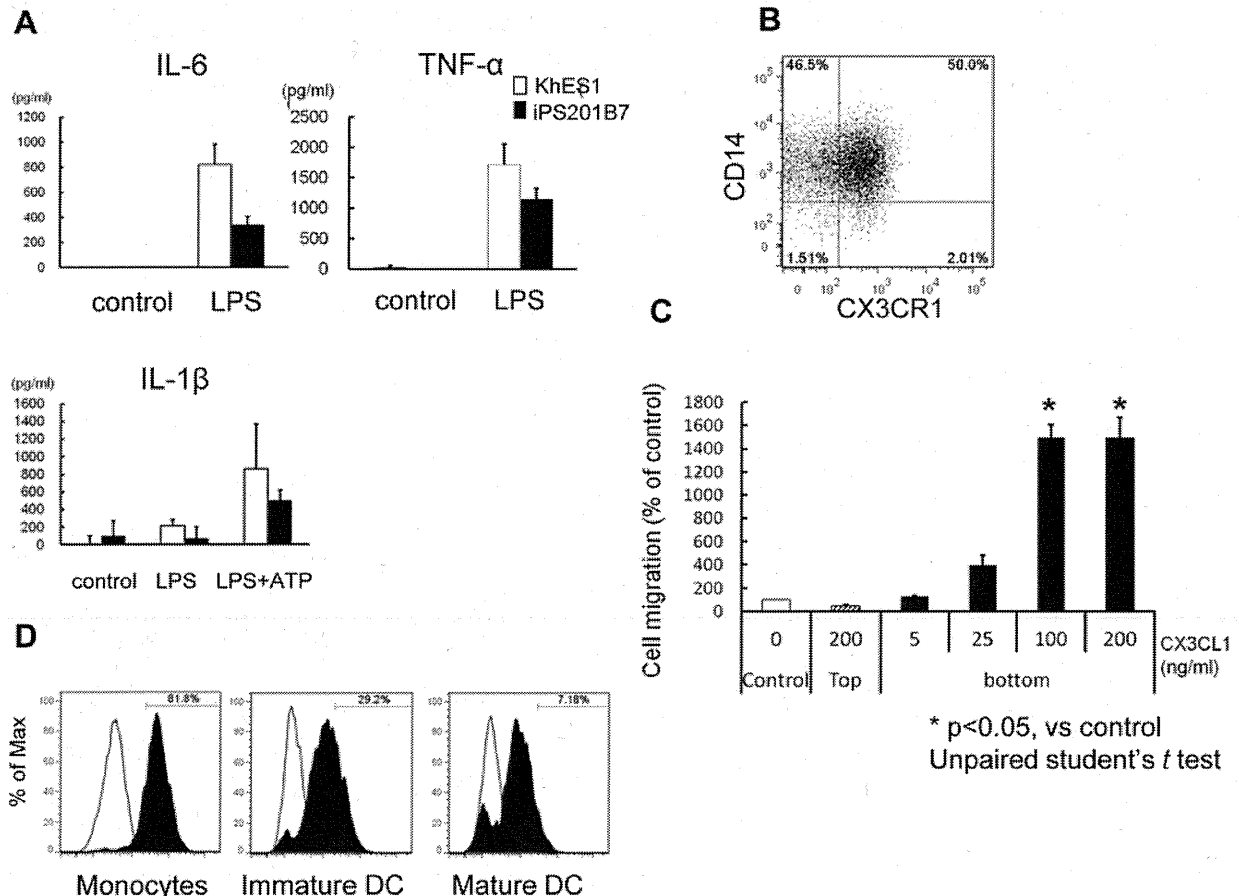


Figure 3. Functional assays for monocytes derived from pluripotent stem cells. (A) The levels of IL-6 and TNF α in supernatants of PS-Mo culture medium 4 hours after LPS stimulation. The levels of IL-1 β were measured 4 hours after LPS stimulation with/without an additional 30-minute ATP stimulation. (B) Flow cytometric analysis of CX3CR1 on PS-Mo. (C) Chemotaxis assay of PS-Mo for CX3CL1 (fractalkine) using a trans-well migration assay. After the addition of CX3CL1 into either the bottom or top of the trans-well chamber, PS-Mo were applied and incubated for 5 hours at 37°C. (D) Antigen uptake was evaluated in monocytes, immature DCs and mature DCs derived from pluripotent stem cells by examining the fluorescence intensity of Alexa fluor 488-conjugated ovalbumin 45 minute after incubation at 37°C (black). Control samples (white) were kept on ice. (B–D) The data of KhES1-derived cells are shown as representative. PS-Mo: monocyte derived from pluripotent stem cells. doi:10.1371/journal.pone.0059243.g003

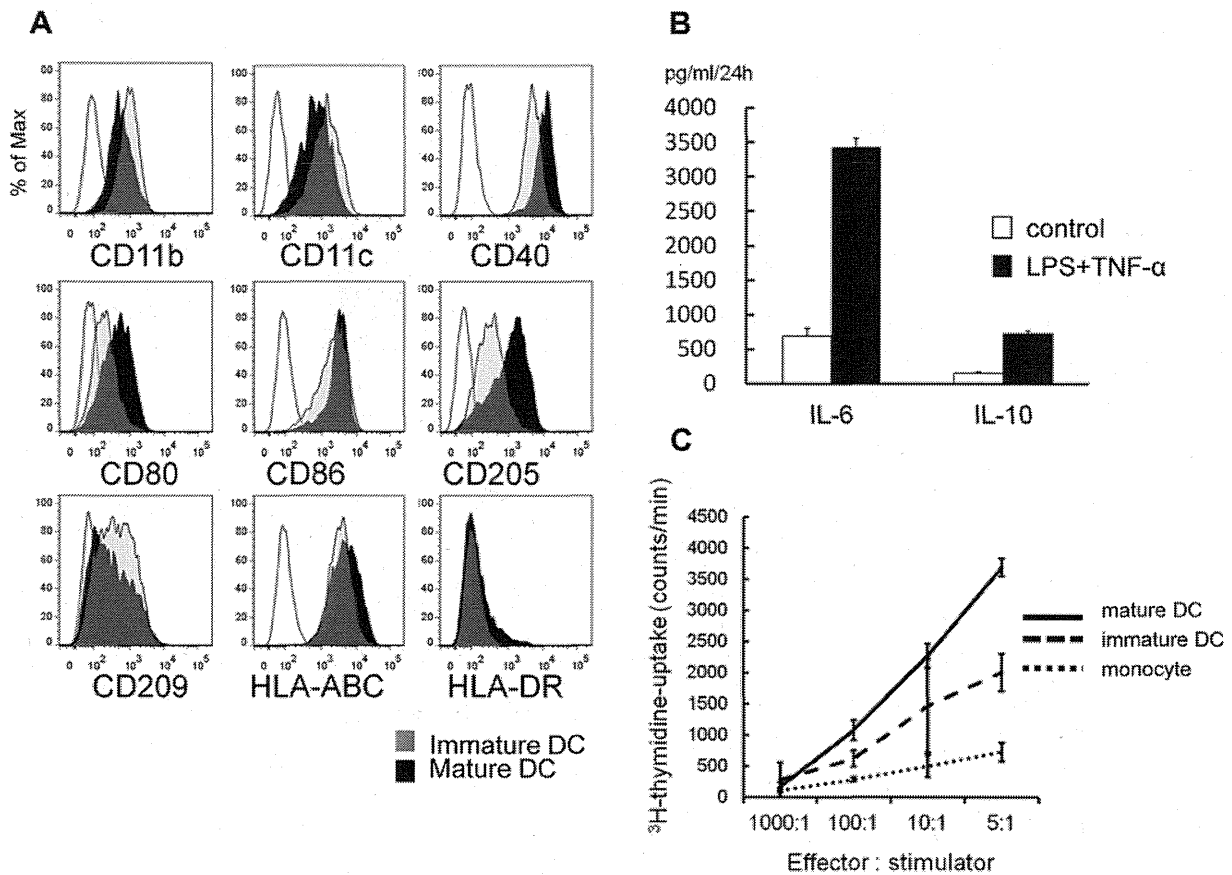


Figure 4. Functional assays for dendritic cells derived from pluripotent stem cells. (A) Flow cytometric analysis of immature/mature DCs derived from pluripotent stem cells. (B) The levels of IL-10 and TNF α in supernatants of culture medium with PS-DCs 24 hours after LPS stimulation. (C) The proliferation of allogeneic naive T cells (1×10^5 cells per well) co-cultured with 40 Gy-irradiated stimulator cells for 3 days was evaluated. The proliferation of naive T cells in the last 16 hours was measured by ^3H -thymidine uptake. (A–C) The data of KhES1-derived cells are shown as representative. doi:10.1371/journal.pone.0059243.g004

fetal bovine serum (FBS) and M-CSF (100 ng/mL) for 7 days with a medium change at day 4, for differentiation into macrophages (step 5-2). IFN γ (20 ng/ml) or IL-4 (20 ng/ml) was added for another day to promote differentiation into M1 or M2 macrophages, respectively.

Flow Cytometric Analysis

Flow cytometric analysis data were collected using the MACS QuantTM Analyzer (Miltenyi Biotec) and then analyzed utilizing the FlowJo software package (Treestar). The following antibodies were purchased from BD Biosciences: CD11b-FITC, CD11c-APC, CD34-PE, CD40-PE, CD43-FITC, CD80-PE, CD83-PE, CD86-FITC, CD205-Alexa fluor 647, CD206-FITC, CD209-PE, HLA-ABC-FITC and HLA-DR-FITC. CD14-APC and CD45-APC antibodies were purchased from Beckman Coulter. CD163-APC antibody was purchased from R&D systems. KDR (CD309)-Alexa fluor 647 and CX3CR1-PE antibodies were purchased from Biolegend.

May-Giemsa Staining and Esterase Staining

Cells were seeded onto glass slides by CYTOSPIN 4 (Thermo Scientific) and stained with May-Grunwald and Giemsa staining

solution (MERCK) and Esterase staining solution (Muto pure chemicals) following the manufacturer's instructions.

RNA Extraction and RT-PCR Analysis

RNA samples were prepared using the RNeasy mini kit (Qiagen) following the manufacturer's instructions. Typically, 500 ng of total RNA were subjected to reverse transcription (RT) with a Sensiscript-RT kit (Qiagen). RT-PCR was performed for the evaluation of the expression of monocytic lineage marker genes such as *PUL1*, *MAF*, *TLR4*, *CCL17* and *CCL18* using the primers in **Table S1**. [21–22] Peripheral blood monocyte-derived mature DCs/macrophages were generated from peripheral CD14⁺ monocytes using the step 5-1/5-2 cytokine cocktails in 10% FBS-supplemented RPMI-1640 for use as positive controls.

Cytokine Assay

Concentrations of cytokines (IL-1 β , IL-6, IL-10, IL-12p70 and TNF α) in supernatants were analyzed with FlowCytomix kits (Bender MedSystems) following the manufacturer's instructions. The IL-1 β , IL-6 and TNF α levels in the culture supernatants of pluripotent cell-derived monocytes (PS-Mo) were analyzed in three settings, (1) culture in RPMI-1640 medium supplemented with 10% FBS and LPS (100 ng/ml) for 4.5 hours, (2) as in (1) but with

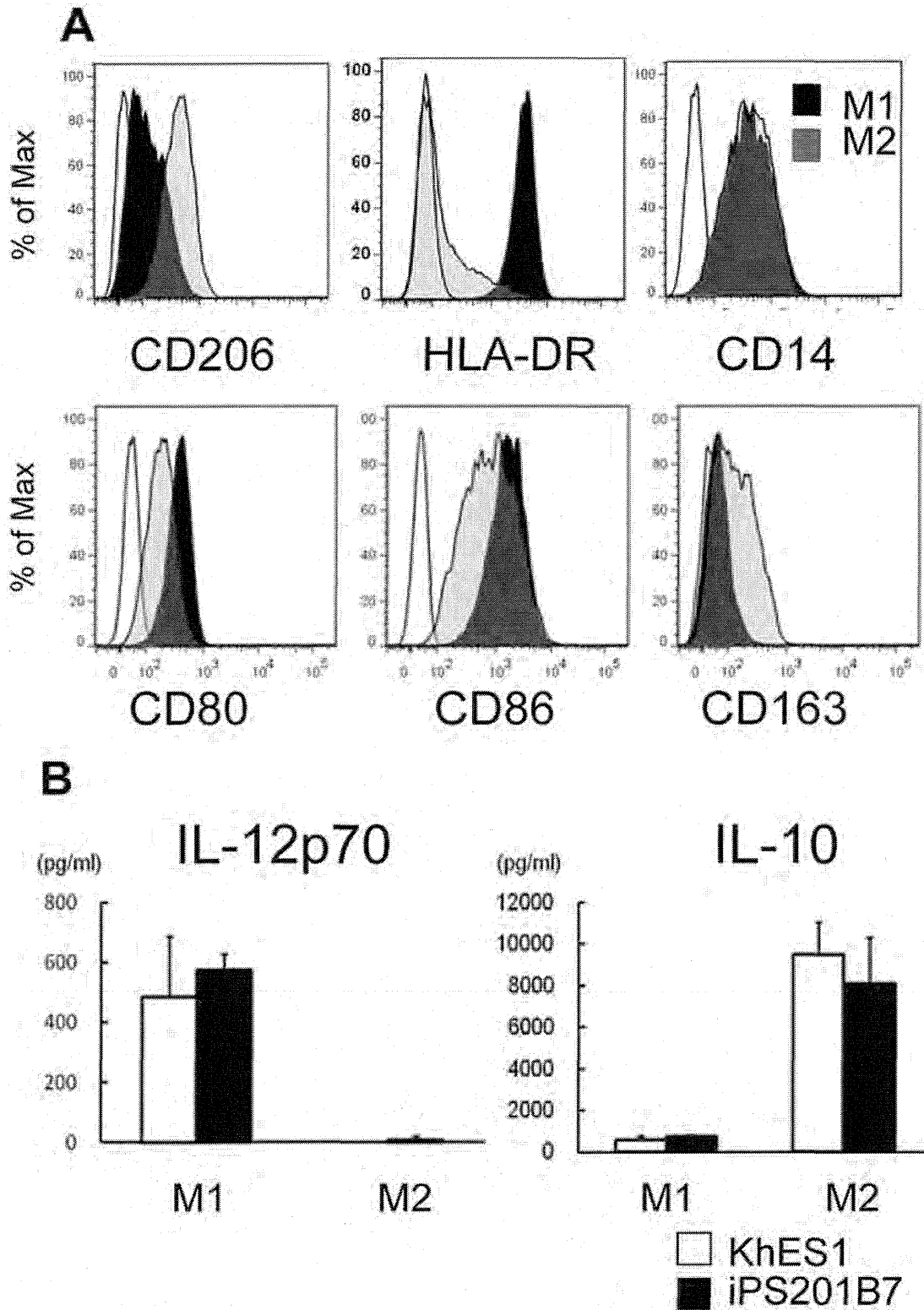


Figure 5. Functional assays for M1/M2 macrophages derived from pluripotent stem cells. (A) Flow cytometric analysis of M1/M2 macrophages derived from pluripotent stem cells. (B) The levels of IL-12p70 and IL-10 in supernatants of culture medium with M1/M2 macrophages derived from pluripotent stem cells 24 hours after LPS stimulation. The data of KhES1-derived cells are shown as representative. doi:10.1371/journal.pone.0059243.g005

the addition of ATP (1 mM) for the last 30 min, (3) without LPS or ATP for 4.5 hours, to evaluate the production pattern of IL-1 β in response to LPS plus ATP. [23].

The levels of IL-6, IL-10, IL-12p70 and TNF α in the supernatants of M1 or M2 macrophage culture were measured 24 hours after LPS (100 ng/ml) stimulation.

Chemotaxis Assay

PS-Mo chemotaxis was evaluated using a trans-well migration assay with 8- μ m pore size inserts (BD Biosciences). After CX3CL1 (fractalkine; R&D systems) was added to either the bottom or top of the chamber, serum-starved PS-Mo were loaded onto the inserts which were placed into 24-well plates containing RPMI-1640 and then incubated at 37°C for 5 hours. [24] Cell migration was measured by flow cytometry as previously reported: equivalent amounts of counting beads were added to each sample and the ratios of PS-Mo to the counting beads were calculated. [25].

Antigen Uptake Assay

The antigen uptake capacity of monocytic lineage cells was evaluated as previously described. [26] Briefly, the cells were collected and stored on ice for 10 min. PS-Mo, pluripotent cell-derived immature DCs (PS-imDCs) and pluripotent cell-derived mature DCs (PS-mDCs) (5×10^4 cells) were incubated with Ovalbumin Alexa fluor 488 Conjugate (Molecular Probes) at 0.1 mg/ml at 37°C or on ice for 45 min. Ice-cold FACS buffer was added in order to stop the reaction, samples washed twice, and the fluorescence intensity analyzed by flow cytometry.

Mixed Leukocyte Reactions

Allogeneic naïve T cells (1×10^5 cells per well) were purified from umbilical cord blood mononuclear cells using naïve CD4⁺ T cell isolation kits (Miltenyi Biotec) and then co-cultured with 40 Gy-irradiated stimulator cells (PS-Mo, PS-imDC, and PS-mDC) in 96-well round bottomed culture plates for 3–5 days. ³H-methylthymidine (25 uCi/ml, Moravak Biochemicals and Radiochemicals) was added to the culture medium of 10% FBS-supplemented RPMI-1640 for the last 16 hours. The cells were harvested onto a filter mat (Perkin Elmer) and the ³H methylthymidine uptake determined using a scintillation counter (MicroBeta TriLux, Perkin Elmer).

Ethical Considerations

This study was approved by the Ethics Committee of Kyoto University and written informed consent was obtained from each healthy volunteer.

Statistics

Data are presented as the mean \pm S.D. and the statistical significance of the differences between cultures were evaluated by Student's *t*-test.

Results

Differentiation of ESCs/iPSCs into Dendritic Cells and Macrophages via Monocyte-like Cells

A KDR⁺CD34⁺ hemangioblast-like population was detected in adherent cell clusters on day 6 (steps 1,2), and around 95% of supernatant cells were CD43⁺CD45⁺ hematopoietic cells on days 13–15 (step 3; **Figure 2A**). [17] Floating cells were recovered every 3–4 days in step 4 (**Figure S1**); the majority of these cells were CD14⁺ monocyte-like cells (**Figure 2A**). These pluripotent cell-derived monocytes (PS-Mo) were similar to

peripheral blood monocytes in morphology (**Figure 2B**). PS-Mo are positive for Esterase staining which was inhibited by NaF (**Figure 2C**). The percentages of PS-Mo in floating cells were constantly about 50–90% between day 18–28 (**Figure 2D and Figure S2A**). The yield of PS-Mo per 100 mm culture dish starting with about 30 colonies was $1.3 \times 10^6 \pm 0.3 \times 10^6$ at each step-4 medium exchange.

To derive DCs, PS-Mo were purified by magnetic sorting, and differentiated into CD14⁺CD83⁺ immature DCs (PS-imDCs) with the step 5-1 cytokine cocktail in 5 days (**Figure 2E**). PS-imDCs were stimulated with LPS and TNF α for an additional 2 days, which further differentiated them into CD14⁺CD83⁺ mature DCs (PS-mDCs) (**Figure 2F**). The differentiation efficiency of mature DCs from PS-Mo was comparable to that from primary monocytes ($7.7\% \pm 0.9\%$ vs. $16.5\% \pm 1.0\%$, $p = 0.20$, unpaired Student's *t*-test). PS-Mo also had the potential to differentiate into macrophages (PS-MPs) with the step 5-2 cytokine cocktail. PS-MPs are morphologically comparable to primary monocyte-derived macrophages and they express typical surface markers such as CD14 and CD68 (**Figure 2G and Figure S3A,B**).

We confirmed that PS-Mo, pluripotent cell-derived DCs (PS-DCs), and PS-MPs expressed monocytic lineage-specific genes (**Figure 2H and Figure S2B**). [22,27] Collectively, by using this protocol, sufficient numbers of monocytic cell lineage cells can be obtained from a small number of human ESCs/iPSCs.

Functional Assays for Monocytes Derived from ESCs/iPSCs

Next, we evaluated the functional activity of pluripotent cell-derived monocytic lineage cells. PS-Mo robustly produced the pro-inflammatory cytokines IL-6 and TNF α after LPS stimulation (**Figure 3A, Figure S3C**). Secretion pattern of IL-1 β from PS-Mo with two stepwise signals LPS and ATP were similar to primary monocytes (**Figure 3A, Figure S3D**). [23,28].

PS-Mo expressed CX3CR1, implying chemotactic responses to CX3CL1 (fractalkine) (**Figure 3B**). PS-Mo migration in trans-well assays increased with increasing doses of CX3CL1 in the lower compartment of the chamber (**Figure 3C**). This phenomenon was not due to chemokinesis, but chemotaxis, because CX3CL1 in the top compartment could not induce PS-Mo migration into the lower compartment of the chamber. [24] We next compared the antigen uptake ability of PS-Mo, PS-imDCs, and PS-mDCs by incubating them with Ovalbumin Alexa fluor 488 Conjugate. [26] PS-Mo had the highest ability to take up antigen and as DCs matured they lost their ability to endocytose antigens (**Figure 3D**).

Functional Assays for DCs Derived from ESCs/iPSCs

For evaluating functions of PS-DCs, we first confirmed that patterns of expression of cell surface markers on PS-imDCs/mDCs were comparable to those on primary dendritic cells (**Figure 4A, Figure S4A**). When stimulated with LPS and TNF α , PS-DCs also produced almost comparable amounts of pro-inflammatory and anti-inflammatory cytokines (**Figure 4B, Figure S4B**).

To test the ability of PS-DCs to activate naïve T cells, we next co-cultured allogeneic naïve T cells with PS-DCs and PS-Mo. As shown in **Figure 4C**, PS-mDCs had the most potent capacity to stimulate allogeneic T cell proliferation and this dose-response relationship was comparable to that observed with PB-DCs (**Figure S4C**).

Functional Assays for Macrophages Derived from ESCs/iPSCs

Using this technique, we obtained morphologically typical macrophage-like cells that adhered firmly to the culture dish. To test whether these PS-MPs possessed functional plasticity like primary macrophages, we tried to polarize them into M1 or M2 state by treating them with IFN γ or IL-4, respectively. PS-MPs exhibited typical surface markers that were characteristic of primary M1 or M2 macrophages (Figure 5A, Figure S5A). The M1 cytokine pattern is typically IL-12^{high} and IL-10^{low}, whereas the M2 pattern is IL-12^{low} and IL-10^{high}. [5] Pluripotent cell-derived M1 and M2 macrophages (PS-M1/M2) also exhibited cytokine profiles that were comparable to those generated from primary monocytes (Figure 5B, Figure S5B).

Discussion

We have established a novel differentiation system for monocytic cells from human ES and iPSC cells. Since macrophages and dendritic cells are usually obtained *in vitro* from monocytes, the most important point of the evaluation is to establish whether monocytes differentiated from ESCs/iPSCs are functionally comparable to primary monocytes. In several functional assays, PS-Mo indeed proved to be comparable to primary monocytes, and importantly, PS-DCs and PC-MPs from PS-Mo were also functionally comparable to their primary counterparts.

Although complete M1/M2 macrophage polarization still requires aserum-containing medium, the present results prove that the current method can precisely manipulate macrophages that have the potential to differentiate into M1/M2 macrophages. The cytokine profiles of PS-M1/M2 were also comparable to those of primary M1/M2 macrophages. The expression patterns of surface markers in PS-DCs after LPS stimulation and of PS-MPs after M1/M2 polarization were almost identical to those of DCs/MP derived from primary monocytes. However, the level of IL-10 in PS-DCs after stimulation was higher than that in primary DCs and the expression levels of HLA-DR in PS-DCs/MP were low in comparison with those in DCs/MP derived from primary monocytes. Therefore, further improvement of culture conditions such as the use of a modified medium and cytokine cocktail will be needed.

Several embryonic body methods and feeder cell co-culture methods for PS-DCs/MP differentiation have already been reported. [7,27,29–30] These methods show relatively poor-reproducibility because of the use of xenogeneic feeder cells and/or serum. In an earlier report which describes a protocol that can derive macrophages and dendritic cells from human iPSCs in feeder- and serum-free manner, [7] the authors did not fully characterize the monocytes and noted that PS-DCs/MP were generated only from two of the five iPSC clones tested. The current culture system simply propagated progenitor cells in 2-dimensional cultures without passage or sorting, and floating PS-Mo and PS-DCs/MP could be obtained repetitively from all five ESC/iPSC clones tested (Figure S2 and S6). These monocytic cells derived from disease- or patient-specific iPSC would be useful tools for the examination of disease pathologies and for drug discovery in immunological disorders such as autoimmune diseases, immunodeficiencies and autoinflammatory syndromes. However, even in our protocol, there are subtle clonal variations of timing of differentiation such as the day of step 3 to 4 switching which is determined by the emergence of CD43⁺CD45⁺ cells (day 13–15, data not shown). Fine adjustment of the protocol for each ESC/iPSC clone seemed to further improve the yield of monocytes.

iPSC technology is overcoming immunological and ethical concerns in regenerative medicine using human pluripotent cells. Furthermore, a number of disease-associated iPSCs generated

from patients with immunological disorders have been reported. [15,31–34] Because patient- or disease-specific iPSC cells will be an important resource for unraveling human immunological disorders, a robust and simple hematopoietic differentiation system that can reliably mimic *in vivo* hematopoiesis is necessary for this purpose. Our simple and robust protocol to produce monocytic cells is therefore expected to be useful for regenerative medicine and studies of immunological disorders.

Supporting Information

Figure S1 Image of floating hematopoietic cells derived from iPSC cells Phase contrast image of floating hematopoietic cells derived from iPSC-201B7 at day 21 (step 4). (PDF)

Figure S2 Phenotype analysis and gene expression pattern of monocytic lineage cells derived from 3 additional pluripotent stem cell lines. (A) The percentage of CD14⁺ cells within the total floating cells derived from 3 iPSC clones (253G4, CIRA188Ai-W2, and CB-A11) was evaluated from day 13 to day 28. (B) RT-PCR analysis of monocytic lineage cells derived from 253G4, CIRA188Ai-W2, and CB-A11 clones for expression of monocytic lineage marker genes (*c-MAF*, *TLR4*, and *CCL17*). Peripheral blood monocytes and peripheral blood monocyte-derived mature DCs were used as positive controls. (PDF)

Figure S3 Characteristics of primary monocytes and macrophages. (A) Phase contrast image and (B) flow cytometric analysis of macrophages derived from primary monocytes. (C) The levels of IL-6 and TNF- α in supernatants of primary monocyte culture medium 4 hours after LPS stimulation. (D) The levels of IL-1 β were measured 4 hours after LPS stimulation with/without an additional 30-minute ATP stimulation. (PDF)

Figure S4 Characteristics and functional assays of dendritic cells derived from primary monocytes. (A) Flow cytometric analysis of immature/mature DCs derived from primary monocytes. (B) The levels of IL-10 and TNF- α in supernatants of culture medium with primary-DCs 24 hours after LPS stimulation. (C) The proliferation of allogeneic naive T cells (1×10^5 cells per well) co-cultured with 40 Gy-irradiated stimulator cells for 3 days was evaluated. The proliferation of naive T cells in the last 16 hours was measured by 3H-thymidine uptake. (PDF)

Figure S5 Characteristics and functional assays of M1/M2 macrophages derived from primary monocytes. (A) Flow cytometric analysis of M1/M2 macrophages derived from primary monocytes. (B) The levels of IL-12p70 and IL-10 in supernatants of culture medium with M1/M2 macrophages derived from primary monocytes 24 hours after LPS stimulation. (PDF)

Figure S6 Replication assays for 3 additional pluripotent stem cell lines. (A) Phase contrast image (left) and May-Giemsa staining (right) of mature DCs derived from iPSC clones. (B) Phase contrast image of macrophages derived from iPSC clones. (C) Flow cytometric analysis of immature/mature DCs and macrophages derived from iPSC clones. (PDF)

Table S1 Primers for RT-PCR. (PDF)

Acknowledgments

We are grateful to Y. Sasaki, Y. Jindai, K. Kobayashi, M. Yamane, and S. Nakamura for technical assistance. We would also like to thank N. Takasu and Y. Takao for administrative assistance.

References

1. Auffray C, Sieweke MH, Geissmann F (2009) Blood monocytes: development, heterogeneity, and relationship with dendritic cells. *Annu Rev Immunol* 27: 669–692.
2. Mosser DM, Edwards JP (2008) Exploring the full spectrum of macrophage activation. *Nat Rev Immunol* 8: 958–969.
3. Geissmann F, Manz MG, Jung S, Sieweke MH, Merad M, et al. (2010) Development of monocytes, macrophages, and dendritic cells. *Science* 327: 656–661.
4. Ingersoll MA, Platt AM, Potteaux S, Randolph GJ (2011) Monocyte trafficking in acute and chronic inflammation. *Trends Immunol* 32: 470–477.
5. Mantovani A, Sozzani S, Locati M, Allavena P, Sica A (2002) Macrophage polarization: tumor-associated macrophages as a paradigm for polarized M2 mononuclear phagocytes. *Trends Immunol* 23: 549–555.
6. Boudreau JE, Bonehill A, Thielemans K, Wan Y (2011) Engineering dendritic cells to enhance cancer immunotherapy. *Mol Ther* 19: 841–853.
7. Senju S, Haruta M, Matsumura K, Matsunaga Y, Fukushima S, et al. (2011) Generation of dendritic cells and macrophages from human induced pluripotent stem cells aiming at cell therapy. *Gene Ther* 18: 874–883.
8. Collin M, Bigley V, Hagiwara M, Hambleton S (2011) Human dendritic cell deficiency: the missing ID? *Nat Rev Immunol* 11: 575–583.
9. Thomson JA, Itskovitz-Eldor J, Shapiro SS, Waknitz MA, Swiergiel JJ, et al. (1998) Embryonic stem cell lines derived from human blastocysts. *Science* 282: 1145–1147.
10. Takahashi K, Tanabe K, Ohnuki M, Narita M, Ichisaka T, et al. (2007) Induction of pluripotent stem cells from adult human fibroblasts by defined factors. *Cell* 131: 861–872.
11. Yamanaka S (2007) Strategies and new developments in the generation of patient-specific pluripotent stem cells. *Cell Stem Cell* 1: 39–49.
12. Orlovskaya I, Schraufstatter I, Loring J, Khaldoyanidi S (2008) Hematopoietic differentiation of embryonic stem cells. *Methods* 45: 159–167.
13. Royer PJ, Tanguy-Royer S, Ebstein F, Sapede C, Simon T, et al. (2006) Culture medium and protein supplementation in the generation and maturation of dendritic cells. *Scand J Immunol* 63: 401–409.
14. Suemori H, Yasuchika K, Hasegawa K, Fujioka T, Tsuneyoshi N, et al. (2006) Efficient establishment of human embryonic stem cell lines and long-term maintenance with stable karyotype by enzymatic bulk passage. *Biochem Biophys Res Commun* 345: 926–932.
15. Tanaka T, Takahashi K, Yamane M, Tomida S, Nakamura S, et al. (2012) Induced pluripotent stem cells from CINCA syndrome patients as a model for dissecting somatic mosaicism and drug discovery. *Blood*.
16. Okita K, Matsumura Y, Sato Y, Okada A, Morizane A, et al. (2011) A more efficient method to generate integration-free human iPS cells. *Nat Methods* 8: 409–412.
17. Niwa A, Heike T, Umeda K, Oshima K, Kato I, et al. (2011) A novel serum-free monolayer culture for orderly hematopoietic differentiation of human pluripotent cells via mesodermal progenitors. *PLoS One* 6: e22261.
18. Pick M, Azzola L, Mossman A, Stanley EG, Elefanti AG (2007) Differentiation of human embryonic stem cells in serum-free medium reveals distinct roles for bone morphogenetic protein 4, vascular endothelial growth factor, stem cell

Author Contributions

iPSC establishment: MDY IA. Conceived and designed the experiments: MDY AN HG TH TN MKS. Performed the experiments: MDY ST SN YM TT JI FHO. Analyzed the data: MDY AN TY KO TN MKS. Wrote the paper: MDY AN TY MKS.

- factor, and fibroblast growth factor 2 in hematopoiesis. *Stem Cells* 25: 2206–2214.
19. Umeda K, Heike T, Yoshimoto M, Shiota M, Suemori H, et al. (2004) Development of primitive and definitive hematopoiesis from nonhuman primate embryonic stem cells in vitro. *Development* 131: 1869–1879.
20. Yu P, Pan G, Yu J, Thomson JA (2011) FGF2 sustains NANOG and switches the outcome of BMP4-induced human embryonic stem cell differentiation. *Cell Stem Cell* 8: 326–334.
21. Friedman AD (2007) Transcriptional control of granulocyte and monocyte development. *Oncogene* 26: 6816–6828.
22. Zhong W, Fei M, Zhu Y, Zhang X (2009) Transcriptional profiles during the differentiation and maturation of monocyte-derived dendritic cells, analyzed using focused microarrays. *Cell Mol Biol Lett* 14: 587–608.
23. Mariathasan S, Weiss DS, Newton K, McBride J, O'Rourke K, et al. (2006) Cryopyrin activates the inflammasome in response to toxins and ATP. *Nature* 440: 228–232.
24. Gevrey JC, Isaac BM, Cox D (2005) Syk is required for monocyte/macrophage chemotaxis to CX3CL1 (Fractalkine). *J Immunol* 175: 3737–3745.
25. Morishima T, Watanabe K, Niwa A, Fujino H, Matsubara H, et al. (2011) Neutrophil differentiation from human-induced pluripotent stem cells. *J Cell Physiol* 226: 1283–1291.
26. Li GB, Lu GX (2010) Adherent cells in granulocyte-macrophage colony-stimulating factor-induced bone marrow-derived dendritic cell culture system are qualified dendritic cells. *Cell Immunol* 264: 4–6.
27. Choi KD, Vodyanik MA, Shukvin II (2009) Generation of mature human myelomonocytic cells through expansion and differentiation of pluripotent stem cell-derived lin-CD34+CD43+CD45+ progenitors. *J Clin Invest* 119: 2818–2829.
28. Hogquist KA, Nett MA, Unanue ER, Chaplin DD (1991) Interleukin 1 is processed and released during apoptosis. *Proc Natl Acad Sci U S A* 88: 8485–8489.
29. Su Z, Frye C, Bae KM, Kelley V, Vieweg J (2008) Differentiation of human embryonic stem cells into immunostimulatory dendritic cells under feeder-free culture conditions. *Clin Cancer Res* 14: 6207–6217.
30. Tseng SY, Nishimoto KP, Silk KM, Majumdar AS, Dawes GN, et al. (2009) Generation of immunogenic dendritic cells from human embryonic stem cells without serum and feeder cells. *Regen Med* 4: 513–526.
31. Jiang Y, Cowley SA, Siler U, Melguizo D, Tilgner K, et al. (2012) Derivation and functional analysis of patient-specific induced pluripotent stem cells as an in vitro model of chronic granulomatous disease. *Stem Cells* 30: 599–611.
32. Park IH, Arora N, Huo H, Maherali N, Ahfeldt T, et al. (2008) Disease-specific induced pluripotent stem cells. *Cell* 134: 877–886.
33. Pessach IM, Ordovas-Montanes J, Zhang SY, Casanova JL, Giliani S, et al. (2011) Induced pluripotent stem cells: a novel frontier in the study of human primary immunodeficiencies. *J Allergy Clin Immunol* 127: 1400–1407 e1404.
34. Zou J, Sweeney CL, Chou BK, Choi U, Pan J, et al. (2011) Oxidase-deficient neutrophils from X-linked chronic granulomatous disease iPS cells: functional correction by zinc finger nuclease-mediated safe harbor targeting. *Blood* 117: 5561–5572.

A Novel Small Compound SH-2251 Suppresses Th2 Cell-Dependent Airway Inflammation through Selective Modulation of Chromatin Status at the *IL5* Gene Locus

Junpei Suzuki^{1,2}, Makoto Kuwahara², Soichi Tofukuji^{2,3}, Masashi Imamura⁴, Fuminori Kato⁴, Toshinori Nakayama^{3,5}, Osamu Ohara², Masakatsu Yamashita^{2,6,7*}

1 Department of Pharmacogenomics, Graduate School of Pharmaceutical Science, Chiba University, Chuo-ku, Chiba, Japan, **2** Department of Human Genome Research, Kazusa DNA Research Institute, Kisarazu, Chiba, Japan, **3** Department of Immunology, Graduate School of Medicine, Chiba University, Chuo-ku, Chiba, Japan, **4** Central Research Institute, Ishihara Sangyo Kaisha, Ltd., Kusatsu, Shiga, Japan, **5** CREST, Japan Science and Technology Agency, Chuo-ku, Chiba, Japan, **6** Department of Immunology, Graduate School of Medicine, Ehime University, Toon, Ehime, Japan, **7** PRESTO, Japan Science and Technology Agency, Toon, Ehime, Japan

Abstract

IL-5 is a key cytokine that plays an important role in the development of pathological conditions in allergic inflammation. Identifying strategies to inhibit IL-5 production is important in order to establish new therapies for treating allergic inflammation. We found that SH-2251, a novel thioamide-related small compound, selectively inhibits the differentiation of IL-5-producing Th2 cells. SH-2251 inhibited the induction of active histone marks at the *IL5* gene locus during Th2 cell differentiation. The recruitment of RNA polymerase II, and following expression of the Th2 cell-specific intergenic transcripts around the *IL5* gene locus was also inhibited. Furthermore, Th2 cell-dependent airway inflammation in mice was suppressed by the oral administration of SH-2251. *Gfi1*, a transcriptional repressor, was identified as a downstream target molecule of SH-2251 using a DNA microarray analysis. The *Gfi1* expression dramatically decreased in SH-2251-treated Th2 cells, and the SH-2251-mediated inhibition of IL-5-producing Th2 cell differentiation was restored by transduction of *Gfi1*. Therefore, our study unearthed SH-2251 as a novel therapeutic candidate for allergic inflammation that selectively inhibits active histone marks at the *IL5* gene locus.

Citation: Suzuki J, Kuwahara M, Tofukuji S, Imamura M, Kato F, et al. (2013) A Novel Small Compound SH-2251 Suppresses Th2 Cell-Dependent Airway Inflammation through Selective Modulation of Chromatin Status at the *IL5* Gene Locus. PLoS ONE 8(4): e61785. doi:10.1371/journal.pone.0061785

Editor: Patricia T. Bozza, Fundação Oswaldo Cruz, Brazil

Received: November 27, 2012; **Accepted:** March 14, 2013; **Published:** April 16, 2013

Copyright: © 2013 Suzuki et al. This is an open-access article distributed under the terms of the Creative Commons Attribution License, which permits unrestricted use, distribution, and reproduction in any medium, provided the original author and source are credited.

Funding: This work was supported by the Global COE Program (Global Center for Education and Research in Immune System Regulation and Treatment), JST PRESTO (Japan), and by grants from the Ministry of Education, Culture, Sports, Science and Technology (Japan) (Grants-in-Aid: Scientific Research (B) #23390075). The funders had no role in study design, data collection and analysis, decision to publish, or preparation of the manuscript.

Competing Interests: The authors have the following interests. Authors MI and FK are employees of Ishihara Sangyo Kaisha, Ltd., the company that provided the SH-2251 (United States Patent No.: US 7632865 B2) for this study. There are no further patents, products in development or marketed products to declare. This does not alter the authors' adherence to all the PLOS ONE policies on sharing data and materials.

* E-mail: yamamasa@m.ehime-u.ac.jp

Introduction

Asthma is a complex chronic inflammatory disease characterized by airway inflammation and hyperresponsiveness obstruction that affects approximately 300 million individuals worldwide [1]. A large number of clinical studies and animal experimental models support a central role of antigen-specific Th2 cells in the pathological responses of atopic asthma [2,3]. In particular, antigen-specific effector and memory Th2 cells appear to play an important role in initiating allergic inflammatory status in the early stage of atopic asthma. Although eliminating Th2 cells and/or inhibiting Th2 cell functions at the early stage of atopic asthma may lead to complete remission, strategies for modulating Th2 cell numbers and/or functions have not been established.

IL-5 is a hematopoietic cytokine that exerts important effects on eosinophils and basophils. IL-5 induces differentiation and maturation of eosinophils in bone marrow, migration to tissue sites and prevention of eosinophil apoptosis [4] [5]. IL-5 also plays a role in the development, metabolism, and function of basophils [6]. Eosinophilic inflammation is a hallmark of asthma that correlates with bronchial hyperresponsiveness and disease severity.

In an asthma model, IL-5-deficient mice did not display eosinophilia, airway hyperreactivity or pulmonary injury, in contrast to that observed in control mice [7]. Treatment of mice with anti-IL-5 mAb also results in decreases in eosinophilic inflammation that are associated with reduced reactivity of methacholine. Therefore, IL-5 is a therapeutic target for allergic inflammation as well as hypereosinophilic syndrome.

Th2 cells produce IL-4, IL-5 and IL-13, and have been shown to play a crucial role in IgE production and eosinophil recruitment. Th2 cells are involved in clearance of extracellular parasites and also promote pathogenic responses associated with allergic inflammation. In peripheral CD4 T cells, IL-4-mediated activation of the transcription factor STAT6 induces the expression of *Gata3* mRNA, which drives Th2 cell differentiation [8]. GATA-3 binds to various regulatory regions on the Th2 cytokine gene loci and induces chromatin remodeling [9,10,11]. In addition, GATA-3 binds to the *IL5* promoter and acts as a transcriptional factor for IL-5 [12].

In addition to Th2 cells, a large number of cell types produce IL-5, including eosinophils [5] [4], natural killer (NK)T cells [13], nuocytes [14], natural helper (NH) cells [15] and IL-5-producing

innate cells [16]. Recently, the IL-33-induced production of IL-5 from innate cells was reported. IL-33-mediated production of IL-5 plays critical roles in lung eosinophil regulation [16], lung inflammation [17] and protease allergen-induced airway inflammation [18]. In addition, the IL-33/IL-5 signaling pathway plays a crucial role in the disease pathogenesis of severe asthma that is resistant to high doses of inhaled corticosteroids but responsive to systemic corticosteroids and anti-IL-5 therapy [19].

Gfi1 is a DNA binding transcriptional repressor that plays important roles in several hematopoietic cells [20]. Gfi1 exerts its role as a transcriptional repressor by interacting with a number of histone modification enzyme including LSD-1/CoRest, G9a and HDACs [21,22,23]. It is well established that Gfi1 regulates the development of Th cell subsets. Zu et al. demonstrated that Gfi1 regulates Th2 cell expansion via enhancement of Stat5 activity [24]. However, the forced expression of constitutively active Stat5 fails to restore Th2 cell development in *Gfi1*-deficient CD4 T cells, possibly because Gfi1 might also play additional roles in Th2 cell development that are independent of Stat5. We previously reported that the expression level of Gata3 proteins and generation of IL-5-producing Th2 cells are severely impaired in *Gfi1*-deficient CD4 T cells [25]. The transduction of Gata3 into *Gfi1*-deficient Th2 cells partially restores the development of IL-5-producing Th2 cells, thus indicating that Gfi1 controls IL-5-producing Th2 cell generation in part through regulation of the Gata3 protein expression.

SH-2251, a thioamide-related compound, was originally synthesized as an inhibitor of IL-5 production. However, the molecular mechanisms by which SH-2251 inhibits IL-5 production and the effects of SH-2251 on Th2 cell differentiation remain to be elucidated. We herein investigated the effects of SH-2251 on Th2 cell differentiation and demonstrated that SH-2251 negatively regulates IL-5-producing Th2 cell differentiation and chromatin remodeling at the *Il5* gene locus. Furthermore, we demonstrated that Th2 cell-dependent allergic airway inflammation is suppressed by oral administration of SH-2251. A DNA microarray analysis revealed that SH-2251 inhibits the differentiation of IL-5-producing Th2 cells via repression of the Gfi1 expression. Therefore, SH-2251 belongs to a unique class of inhibitors of Th2-dependent immune responses that modulate chromatin remodeling at the *Il5* gene locus and the subsequent the differentiation of IL-5 producing Th2 cells.

Results

SH-2251 selectively inhibits the generation of IL-5-producing Th2 cells

SH-2251 (**Fig. 1A**), a novel thioamide-related compound, was originally synthesized as an inhibitor of IL-5 production. However, the effects of SH-2251 on Th2 cell differentiation were not determined. To assess the effects of SH-2251 on Th2 cell differentiation, naïve CD4 T cells were purified and cultured under Th2-conditions in the presence or absence of SH-2251 for five days, and the ability to produce Th2 cytokines was determined using intracellular staining. As shown in **Fig. 1B**, the generation of IL-5-producing Th2 cells decreased in the SH-2251-treated cultures, whereas the number of IL-4- and IL-13-producing cells slightly increased. The selective reduction of IL-5 production was also confirmed on ELISA (**Fig. 1C**). The generation of IFN- γ -producing Th1 cells and IL-17A-producing Th17 cells was moderately decreased, while development of IL-9-producing Th9 cells was augmented by treatment with SH-2251 (**Fig. S1A–C in File S1**). To determine the optimal concentration for inhibition of IL-5-producing Th2 cell differentiation, naïve CD4 T

cells were cultured under Th2-conditions in the presence of the indicated concentrations of SH-2251. Inhibitory effects were observed at the 10 nM concentration of SH-2251 and peaked at 100 nM (**Fig. 1D**). Dose-dependent effects of SH-2251 on the inhibition of IL-5 induction were also confirmed using ELISA (**Fig. 1E**). The production of IL-4 and IL-13 was not impaired (**Fig. 1E**). These results indicate that SH-2251 inhibits IL-5-producing Th2 cell differentiation without inhibiting the generation of IL-4- or IL-13-producing Th2 cells.

SH-2251 selectively inhibits induction of active histone modifications at the *Il5* gene locus during Th2 cell differentiation

Changes in histone modification are a marker of chromatin remodeling [26,27]. During Th2 cell differentiation, active histone modifications including histones H3K4me2/3, H3K9ac and H3K27ac, are induced at Th2 cytokine gene loci [9] [11]. We examined the effect of SH-2251 on the induction of active histone modifications during Th2 cell differentiation. As shown in **Fig. 2A**, the levels of active histone modifications such as those of H3K4me3, H3K9ac and H3K27ac at the *Il5* promoter were reduced by treatment with SH-2251 in a dose-dependent manner. The levels of H3K9ac and H3K27ac, but not H3K4me3, at the *Rad50* promoter decreased (**Fig. 2A**). In sharp contrast, the active histone modifications at the *Il4* and *Il13* promoters were unaffected by SH-2251 treatment (**Fig. 2A**). To confirm the selective effects of SH-2251 on the levels of active histone modifications around the *Il5* gene locus, we performed ChIP-sequencing with anti-histone H3K4me3 pAb and H3K27ac pAb. Decreased levels of H3K4me3 and H3K27ac were detected from the 5' region of the *Rad50* gene to the *Il5* gene, while reduced levels were spread over the down stream region of the *Il5* gene locus in the SH2251-treated Th2 cells (**Fig. 2B and Fig. S2 in File S1**). Reduction in the levels of H3K4me3 and H3K27ac around the *Il5* gene locus in the SH-2251-treated Th2 cells were confirmed using a manual ChIP analysis (**Fig. 2C**). Changes in other histone modifications, including H3K4me2, H3K9me2, H3K36me3 and H3K9ac, around the *Il5* gene locus were also determined with a manual ChIP analysis. The levels of active histone marks such as those of H3K4me2, H3K36me3 and H3K9ac around the *Il5* gene locus were decreased in the SH-2251-treated Th2 cells (**Fig. 2C**). The level of H3K9me2 was not affected by treatment with SH-2251 (**Fig. 2C**). No obvious signals were detected with an anti-H3K27me3 pAb (data not shown). Finally, we assessed the effects of SH-2251 treatment on the recruitment of RNA polymerase II (PolII) and subsequent intergenic transcription around the *Il5* gene locus. SH-2251 reduced the recruitment of polII (**Fig. 2D upper panel**) and the level of transcription (**Fig. 2D lower panel**) in the Th2 cells. These results suggest that SH-2251 blocks the generation of IL-5-producing Th2 cells, presumably by inhibiting chromatin remodeling at the *Il5* gene locus.

Th2-dependent airway inflammation is attenuated by the administration of SH-2251

We next investigated the effects of the oral administration of SH-2251 (10 mg/kg) in mice model of airway inflammation. BALB/c mice were immunized with OVA absorbed by alum, then challenged with OVA intranasally. We observed decreases in the infiltration of inflammatory cells, including eosinophils, in the bronchoalveolar lavage (BAL) fluid of the OVA-immunized SH-2251-treated mice in comparison to that observed in the vehicle-administrated control group (**Fig. 3A**). The expressions of *Il4*, *Il5*

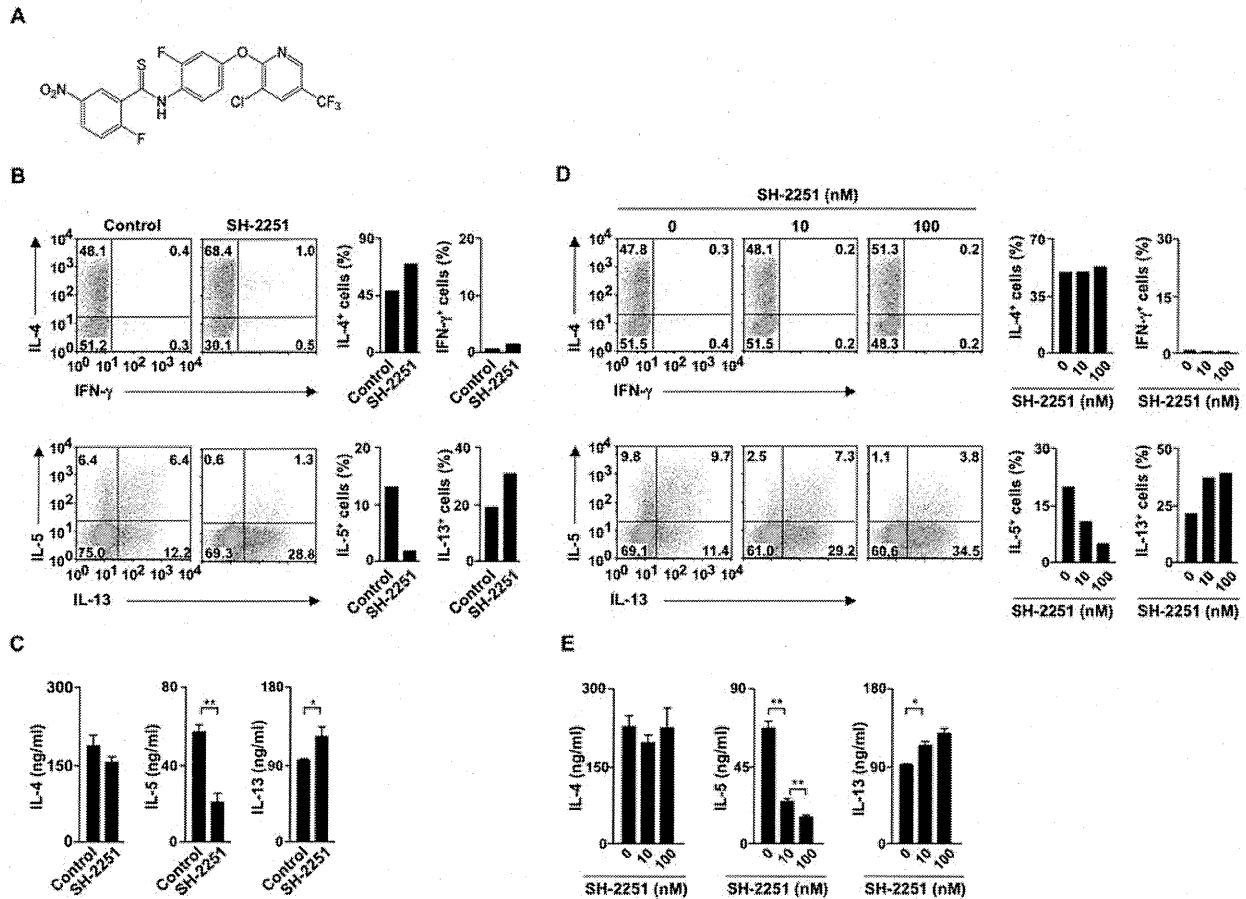


Figure 1. SH-2251 inhibits the generation of IL-5-producing Th2 cells. (A), The chemical structure of SH-2251. **(B),** Naïve CD4 T cells were cultured under Th2-conditions in the presence or absence of SH-2251 (100 nM) for five days. The cells were restimulated with an immobilized anti-TCR- β mAb for six hours, and the intracellular staining profiles of IL-4/IFN- γ (upper panel) and IL-5/IL-13 (lower panel) were determined using intracellular staining, respectively. The percentages of each quadrant are indicated. The average percentages of the generated cytokine-producing cells of three independent experiments are also shown with the standard deviation (right). **(C),** Cytokine production induced by the SH-2251-treated Th2 cells shown in panel (B) was determined with ELISA. **(D),** Naïve CD4 T cells were cultured under Th2-conditions in the presence of the indicated concentrations of SH-2251 for five days. The intracellular profiles were determined as described (B). The average percentage of three independent experiments of the generated cytokine-producing cells are also shown with the standard deviation **(E),** Cytokine production by the SH-2251-treated Th2 cells shown in panel (D) was determined with ELISA. * $P < 0.05$ and ** $P < 0.01$ (Student's t -test). Three independent experiments (C and E) were performed with similar results.

doi:10.1371/journal.pone.0061785.g001

and *Il13* mRNA in the BAL fluid cells were also very low, whereas the reduction of *Ifng* was marginal in the SH-2251-administered group (Fig. 3B). A reduced expression of *eosinophil peroxidase (Epo)* mRNA in the BAL fluid cells of the SH-2251-administered mice supported decreased infiltration of eosinophils (Fig. S3A in File S1). We prepared CD4 T cells from the lungs of OVA-challenged mice to confirm the effects of SH-2251 administration. The expressions of mRNA for Th2 cytokines in the CD4 T cells purified from the lung tissue were reduced in the SH-2251-treated mice (Fig. 3C). The purified CD4 T cells were further stimulated with immobilized anti-TCR- β mAb for 48 hours *in vitro*, and the production of cytokines was determined using ELISA. The level of IL-5 production was low in the CD4 T cells obtained from the SH-2251-administered mice in comparison to that observed in the CD4 T cells obtained from the vehicle-treated mice (Fig. 3D). In addition, the productions of IL-4 and IL-13 were also significantly decreased in the lung CD4 T cells obtained from the SH-2251-treated mice, whereas the IFN- γ production was increased

(Fig. 3D). The number of mononuclear cells infiltrating the peribronchiolar regions of the lungs was reduced by SH-2251 administration (Fig. 3E). Both mucus hyper-production and goblet cell metaplasia, as assessed with PAS staining, were lower in the bronchioles of the SH-2251-administered mice compared to that observed in bronchioles of the vehicle-treated control mice (Fig. 3F). The serum levels of anti-OVA immunoglobulin were unaffected by the administration of SH-2251 (Fig. S3B in File S1). These results indicate that the oral administration of SH-2251 can suppress Th2 cell-mediated allergic airway inflammation.

The expression and functions of Gata3 are not influenced by SH-2251 treatment

Gata3 plays an essential role in the induction of chromatin remodeling at the Th2 cytokine gene locus following Th2 cell differentiation [9] [10] [11]. In addition, Gata3 induces the transcriptional activation of the *Il5* gene [12]. In this study,

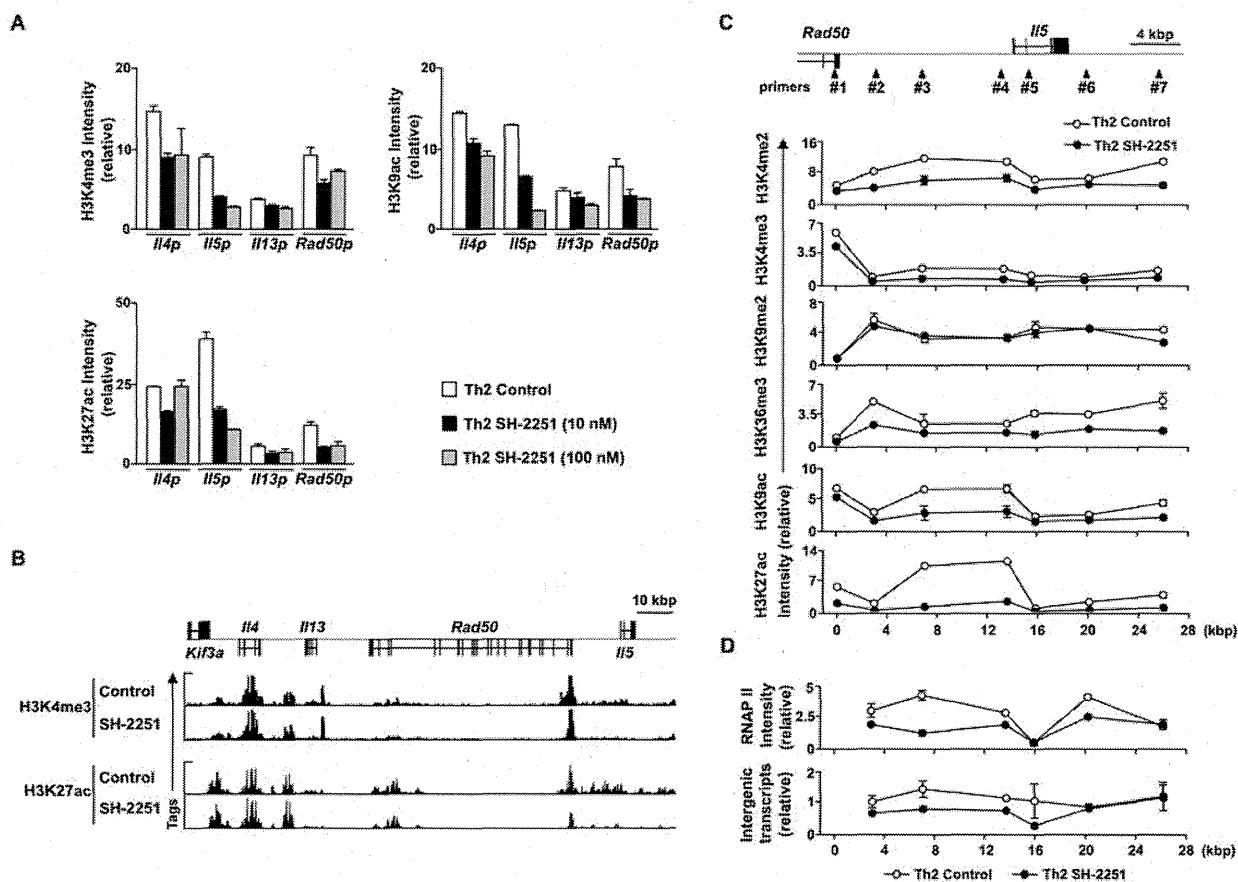


Figure 2. The induction of active histone marks at the *Il5* gene locus is inhibited by SH-2251. (A), Naïve CD4 T cells were cultured under Th2-conditions for five days in the presence of the indicated concentration of SH-2251, and a ChIP assay was performed with the indicated antibodies. The relative intensity (*I*/Input) is shown with the standard deviation. **(B)**, The global patterns of histones H3K4me3 and H3K27ac at the Th2 cytokine gene loci were determined using ChIP-seq. **(C)**, The indicated histone modification status around the *Il5* gene locus in the SH-2251-treated Th2 cells was determined using a manual ChIP assay. The relative intensity (*I*/Input) is shown with the standard deviation. **(D)**, Recruitment of RNA polymerase II around the *Il5* gene locus (upper panel) was determined using a manual ChIP assay. The relative intensity (*I*/Input) is shown with the standard deviation. The transcripts around the *Il5* gene in the SH-2251-treated Th2 cells (lower panel) were determined using quantitative RT-PCR. The relative intensity (*I*/*Hprt*) is shown with the standard deviation. Four independent experiments (A, C and D) were performed with similar results. doi:10.1371/journal.pone.0061785.g002

treatment with SH-2251 showed no effects on the Gata3 mRNA (Fig. 4A) or protein (Fig. 4B) expressions in the Th2 cells. Next, we wanted to determine the effects of SH-2251 on binding of Gata3 at the Th2 cytokine gene locus. The binding of Gata3 throughout the Th2 cytokine gene locus was determined comprehensively using ChIP-seq with an anti-Gata3 pAb. Gata3 has been reported to bind to the V_A enhancer [28], *Il4* intron2 [29], CGRE [30], Th2 LCR [31,32] and *Il5* promoter regions [33] in Th2 cells. The binding of Gata3 at these regions was confirmed with ChIP-seq (Fig. 4C upper panel). In addition, we newly identified several Gata3 binding genomic regions around the *Il5* gene locus (Fig. 4C lower panel: #1~#7). The binding of Gata3 at these regions in the Th2 cells was not inhibited by SH-2251 treatment (Fig. 4D). Finally, we examined whether SH-2251 can inhibit the Gata3-induced transcriptional activation of the *Il5* promoter using a reporter gene analysis. As indicated in Fig. 4E, SH-2251 showed only marginal effects on the Gata3-dependent activation of the *Il5* promoter. These data suggest that Gata3 is unlikely to be a target

of SH-2251 in the inhibition of IL-5-producing Th2 cell development.

A decreased expression of *Gfi1* is involved in the SH-2251-mediated inhibition of IL-5-producing Th2 cell generation

We conducted a DNA microarray analysis to identify the target gene(s) that are involved in the SH-2251-mediated inhibition of IL-5-producing Th2 cell generation. We found that the expression of *Gfi1* mRNA was dramatically decreased in the SH-2251-treated Th2 cells (Fig. 5A). A reduction in the *Gfi1* protein expression was also induced by SH-2251-treatment (Fig. 5B). To assess the molecular mechanisms by which SH-2251 inhibits the *Gfi1* expression, the histone modifications present at the *Gfi1* gene locus were determined using ChIP-seq with an anti-histone H3K27ac pAb or an H3K4me3 pAb, respectively. As shown in Fig. 5C lower panel, a striking reduction in the histone H3K27ac level at the *Gfi1* gene locus in the SH-2251-treated Th2 cells was detected. The level of H3K4me3 at the *Gfi1* gene locus was moderately decreased (Fig. 5C upper panel). A

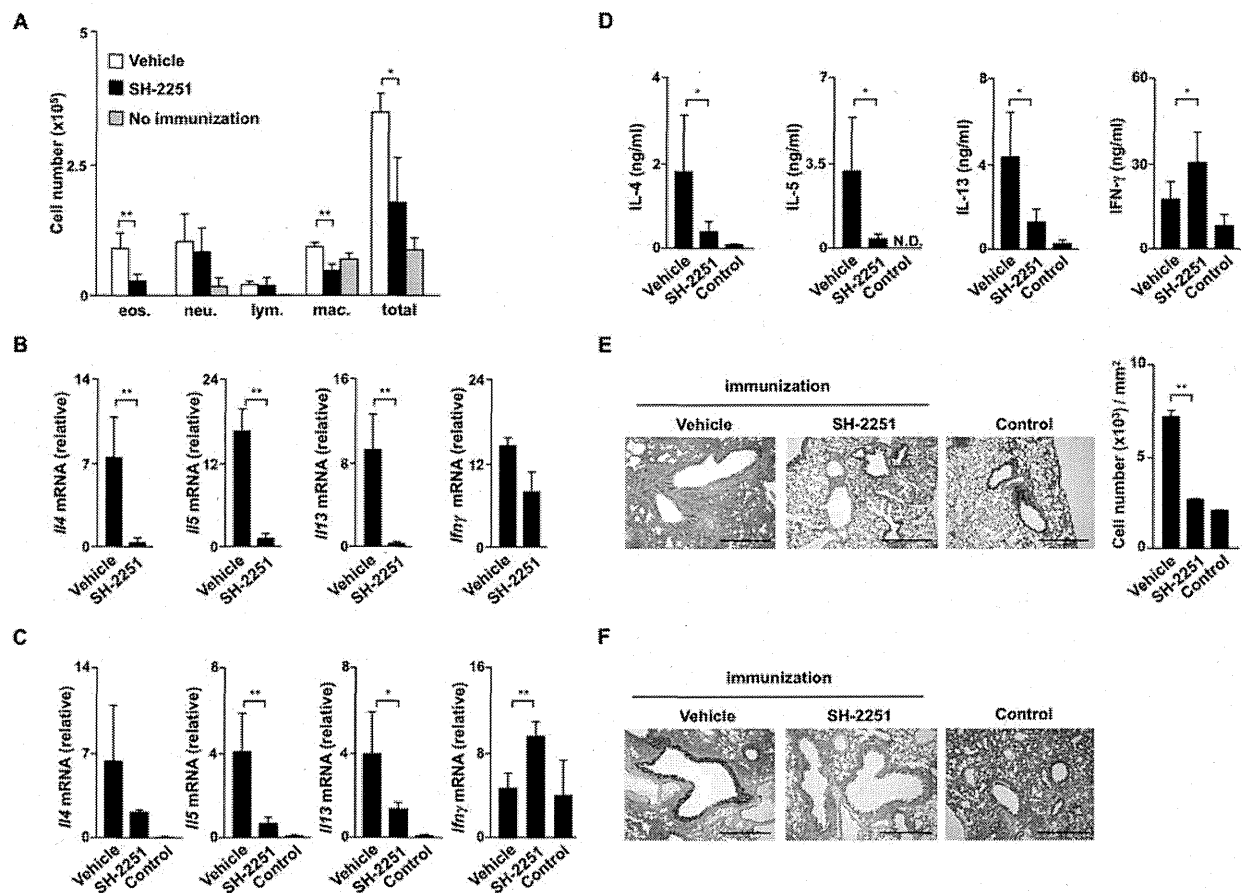


Figure 3. OVA-induced airway inflammation is attenuated by oral administration of SH-2251. (A), Decreased infiltration of eosinophils in the BAL fluid of asthmatic SH-2251-administered mice. The absolute numbers of eosinophils (Eos.), neutrophils (Neu.), lymphocytes (Lym.) and macrophages (Mac.) in the BAL fluid are shown with standard deviations ($n = 5$ per group). $*P < 0.01$ and $**P < 0.001$ by ANOVA and the Bonferroni-test. (B), Quantitative RT-PCR of *Il4*, *Il5* and *Il13* mRNA in the BAL fluid cells of vehicle and SH-2251-administered mice. (C), Quantitative RT-PCR of *Il4*, *Il5*, *Il13* and *Ifn γ* mRNA in the lung CD4 T cells of vehicle and SH-2251-administered mice. ($n = 5$ per group). (D), Cytokine production from lung CD4 T cells of vehicle and SH-2251-administered mice stimulated *in vitro*. The lung CD4 T cells were stimulated with immobilized anti-TCR- β mAb for 48 hours and the concentrations of cytokines in the culture supernatants were determined using ELISA. The lungs were fixed and stained with hematoxylin and eosin (E, left) or periodic acid-Schiff reagent (F, left). The scale bars represent 500 μm . The numbers of infiltrated leukocytes in the peribronchiolar regions are shown (mean cell numbers/ mm^2) (E, right). Three independent experiments were performed with similar results. Student's *t*-test was used for the statistical analyses. $*P < 0.05$ and $**P < 0.01$ (B, C, D and E) doi:10.1371/journal.pone.0061785.g003

dose-dependent inhibition of the H3K4me3 and H3K27ac levels at the *Gfi1* gene locus induced by SH-2251 was confirmed using a manual ChIP assay (Fig. 5D). The level of H3K9ac at the *Gfi1* gene locus was also inhibited by SH-2251 treatment (Fig. 5D). As indicated in Fig. S4 in File S1, the levels of histone H3K27ac and H3K4me3 at the *Gfi1* gene locus were higher in the Th2 cells than that in the naïve CD4 T cells. The levels of histone H3K27ac and H3K4me3 modifications in the SH-2251-treated Th2 cells were almost comparable to those in the naïve CD4 T cells (Fig. S4 in File S1), thus indicating that SH-2251 inhibits the induction of the histone H3K27ac at the *Gfi1* locus during Th2 cell differentiation.

Transduction of *Gfi1* into SH-2251-treated Th2 cells restores IL-5 production

To elucidate the role of *Gfi1* reduction in the SH-2251-mediated inhibition of IL-5-producing Th2 cell differentiation, we transduced *Gfi1* into SH-2251-treated Th2 cells using retrovirus

vectors and measured the IL-5 production ability. As shown in Fig. 6A, the transduction of *Gfi1* into the SH-2251-treated Th2 cells partially restored the generation of IL-5 producing Th2 cells. The production levels of IL-5 in the SH-2251-treated Th2 cells were completely restored by the transduction of *Gfi1* (Fig. 6B). The production of IL-4 and IL-13 in the *Gfi1*-transduced Th2 cells was not altered in comparison to that observed in the Mock-transduced SH-2251-treated Th2 cells (Fig. 6B). The levels of histone H3K4me3 and H3K27ac around the *Il5* gene locus were also ameliorated in the *Gfi1*-transduced SH-2251-treated Th2 cells (Fig. 6C). Histones H3K4me3, H3K9ac and H3K27ac at the *Il4* and *Il13* promoters were not influenced by the transduction of *Gfi1* (Fig. S5 in File S1). To examine the molecular mechanisms by which *Gfi1* controls the histone modification status at the *Il5* gene locus, the binding of *Gfi1* around the *Il5* gene locus was determined using a ChIP-sequence analysis with an anti-*Gfi1* pAb. Low, but reproducible binding of *Gfi1* was detected around the *Il5* gene locus in the Th2 cells (Fig. 6D). The binding of *Gfi1* around

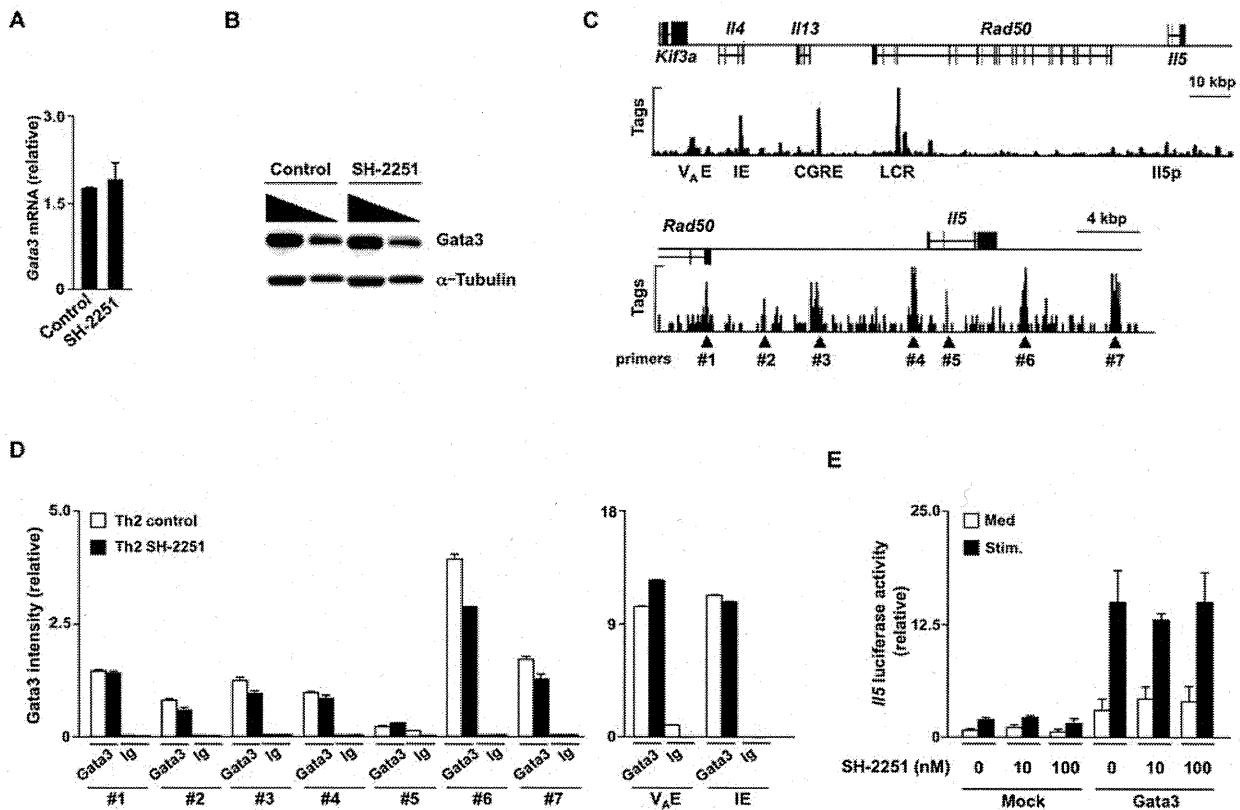


Figure 4. The expression and functions of Gata3 are not impaired by treatment with SH-2251. (A), The mRNA expression of Gata3 in the SH-2251-treated Th2 cells was determined using quantitative RT-PCR. The relative intensity (*/Hprt*) is shown with the standard deviation. (B), The protein expression level of Gata3 was determined with immunoblotting. The nuclear (Gata3) and cytoplasmic (α -Tubulin) lysates with a three fold serial dilution were used. Three independent experiments (A and B) were performed with similar results. (C), The global patterns of Gata3 binding at the Th2 cytokine gene loci (upper panel) and the *IL5* gene locus (lower panel) were determined using ChIP-seencing with an anti-Gata3 pAb. The locations of PCR primer pairs (triangle) used in a manual ChIP assay are also listed. (D), The binding of Gata3 around the *IL5* gene locus (left panel) and the *IL4* gene locus (right panel) in the SH-2251-treated Th2 cells was determined using a manual ChIP assay. The relative intensity (*/Input*) is shown with the standard deviation. Three independent experiments were performed with similar results. (E), The effects of SH-2251 on the Gata3-dependent transcriptional activation of the *IL5* promoter were determined using a Dual luciferase assay. The mean and standard deviation of the relative luciferase activity of three different experiments are shown. Stim: PMA (30 ng/ml)+dbcAMP (100 μ M). Four independent experiments (A, B, D and E) were performed with similar results. doi:10.1371/journal.pone.0061785.g004

the *IL5* gene locus in the Th2 cells decreased by the treatment with SH-2251 (Fig. 6E). These results suggest that SH-2251 inhibits the chromatin remodeling at the *IL5* gene locus and subsequent IL-5-producing Th2 cell differentiation in part by attenuating the Gfi1 expression.

Discussion

We herein demonstrated that a thioamide-related small chemical compound, SH-2251, inhibits the differentiation of IL-5-producing Th2 cells by attenuating the Gfi1 expression. Treatment of developing Th2 cells with SH-2251 reduced the generation of IL-5-producing Th2 cells and the expression of Gfi1. SH-2251 also inhibited induction of active histone modifications at the *IL5* gene locus as well as the *Gfi1* locus in developing Th2 cells. We found that Gfi1 binds to several genomic regions around the *IL5* gene locus in Th2 cells, which was reduced by treatment with SH-2251. We previously reported that the induction of histones H3K4me3 and H3K9/14ac at the *IL5* gene locus and subsequent IL-5-producing Th2 cell differentiation are impaired in *Gfi1*-

deficient CD4 T cells [25]. In addition, in this study, retrovirus vector-mediated transduction of *Gfi1* into SH-2251-treated developing Th2 cells restored the levels of active histone modifications at the *IL5* gene locus, and subsequent generation of IL-5-producing Th2 cells. Therefore, the *Gfi1-IL5* axis is a target for SH2251-mediated inhibition of IL-5-producing Th2 cell differentiation.

Clinical trials of the anti-IL-5 mAb have demonstrated therapeutic benefits across a spectrum of eosinophil-related disorders [34]. Recently, a result of a clinical trial of a humanized anti-IL-5 mAb (Mepolizumab) was reported [35]. Although no changes in airway hyperresponsiveness were noted, reductions in blood/sputum eosinophilia and the number of asthma exacerbations occurring during the year were reported. In addition, reductions in airway wall thickness were also observed. These results indicate that the neutralization of IL-5 might have a positive impact on airway remodeling. We demonstrated the inhibitory effects of SH-2251 on the generation of IL-5-producing Th2 cells and IL-5 production. Furthermore, the oral administration of SH-2251 was found to suppress OVA-induced allergic airway inflammation in a mice model. These data suggest that SH-

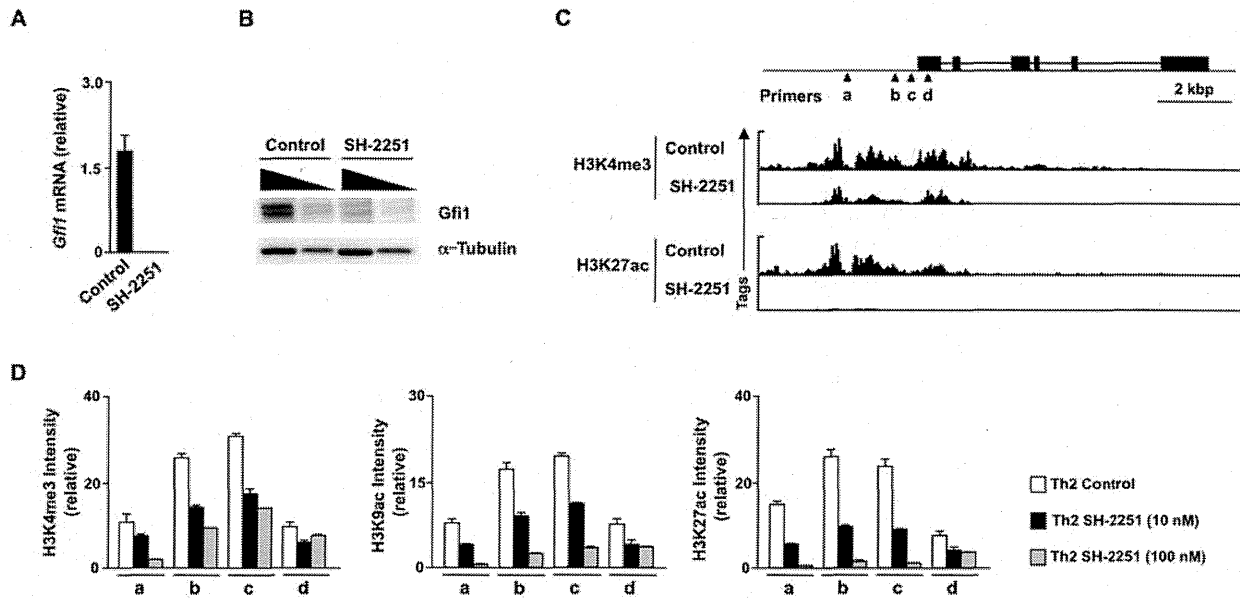


Figure 5. Gfi1 is a downstream target of SH-2251. (A), A decreased *Gfi1* mRNA expression in the SH-2251 treated Th2 cells. The expression of *Gfi1* was determined with quantitative RT-PCR. The relative intensity (*Hprt*) is shown with the standard deviation. **(B),** A decreased level of Gfi1 proteins was detected with immunoblotting. The nuclear (Gfi1) and cytoplasmic (α -Tubulin) lysates with a three fold serial dilution were used. **(C),** The global patterns of the histone H3K4me3 and H3K27ac levels at the *Gfi1* gene locus were determined using ChIP-sequencing. The locations of PCR primer pairs (triangle) used in a manual ChIP assay are also listed. **(D),** Manual ChIP assays were performed with anti-histone H3K4me3, H3K9ac or H3K27ac pAb. The relative intensity (*Input*) is shown with the standard deviation. Four independent experiments (A, B and D) were performed with similar results.
doi:10.1371/journal.pone.0061785.g005

2251 is a novel therapeutic candidate for diseases involving allergic inflammation, including asthma.

The generation of IL-13-producing cells and IL-13 production were augmented by SH-2251 treatment *in vitro*. The IL-13 production moderately increased in the *Gfi1*-deficient CD4 T cells (M.Y. unpublished observation), suggesting that Gfi1 may inhibit IL-13 production in CD4 T cells. However, our *in vivo* experimental results demonstrated a reduction in IL-13 production induced by the administration of SH-2251. In addition, the production of IL-4 was also moderately decreased *in vivo*. A DNA microarray analysis indicated a reduced expression of *Ccr3* mRNA in the SH-2251-treated Th2 cells. Therefore, it is likely that SH-2251 exerts some effects on the expressions of chemokine receptors in Th2 cells and that recruitment of Th2 cells to the inflamed sites is inhibited. In addition, it is possible that SH-2251 also affects the function of antigen-presenting cells. Taken together, although an SH-2251-mediated increase in IL-13 production was detected in the *in vitro* experiments, the administration of SH-2251 provides beneficial effects in the treatment of asthmatic patients.

Lung epithelial cells can produce multiple cytokines, including IL-25 and IL-33, in response to various stressors. The intranasal administration of IL-25 induces asthmatic symptoms [36], and anti-IL-25 antibody treatment suppresses OVA-induced allergic inflammation [37]. It is thought that IL-25 acts on NKT cells and promotes Th2 cytokine production [38]. Recently, the IL-33-mediated production of IL-5 has been reported to play a critical role in lung eosinophil regulation [16], lung inflammation [17] and protease allergen-induced airway inflammation [18]. Gfi1, a downstream target of SH-2251, is broadly expressed in hematopoietic lineage cells, and *Gfi1* knockout animals display many abnormalities, including neutropenia, T cell development defects, hematopoietic stem cell defects and defects in dendritic cell

development and functions [20]. It is likely that Gfi1 is also expressed in NKT cells, NH cells, neutocytes and IL-5-producing innate cells. Therefore, it is interesting to examine whether the treatment of SH-2251 can inhibit both the IL-25- and IL-33-induced production from these cell populations.

SH-2251 inhibits the generation of IL-5-producing Th2 cells, in part by repressing Gfi1 induction. Gfi1 is induced by the TCR-mediated activation of the ERK MAPK cascade [25]. In this study, although SH-2251 inhibited the Gfi1 expression, the inhibitory activity for ERK MAPK was very weak ($IC_{50} > 1 \mu M$; M.I. and F.K. personal communication). The activation of the Ras-ERK MAPK cascade also prevents the ubiquitin/proteasome-dependent degradation of Gata3 [39]. The treatment of developing Th2 cells with SH-2251 failed to inhibit the Gata3 protein expression. Therefore, it is unlikely that SH-2251 inhibits IL-5-producing Th2 cell differentiation by suppressing Ras-ERK MAPK cascade activation.

Gfi1 is a DNA binding transcriptional repressor that interacts with a number of histone modification enzymes, including LSD-1/CoRest [22], G9a [23] and HDACs [21]. However, these histone modification enzymes introduce repressive marks on the histones. We previously demonstrated that Gfi1 is required for induction of active histone marks on the *Il5* gene locus [25]. In addition, the transduction of Gfi1 into SH-2251-treated Th2 cells restored active histone modifications (H3K4me3, H3K9ac and H3K27ac) at the *Il5* gene locus. Although precious molecular mechanisms remain to be elucidated, our data indicate the possible role of Gfi1 in the formation of the active chromatin status.

An increased activity of histone acetyltransferases (HATs) and concomitant reductions in histone deacetylase (HDAC) activity have been reported in asthmatic patients [40] [41]. Changes in these histone modification enzymes result in hyperacetylations of

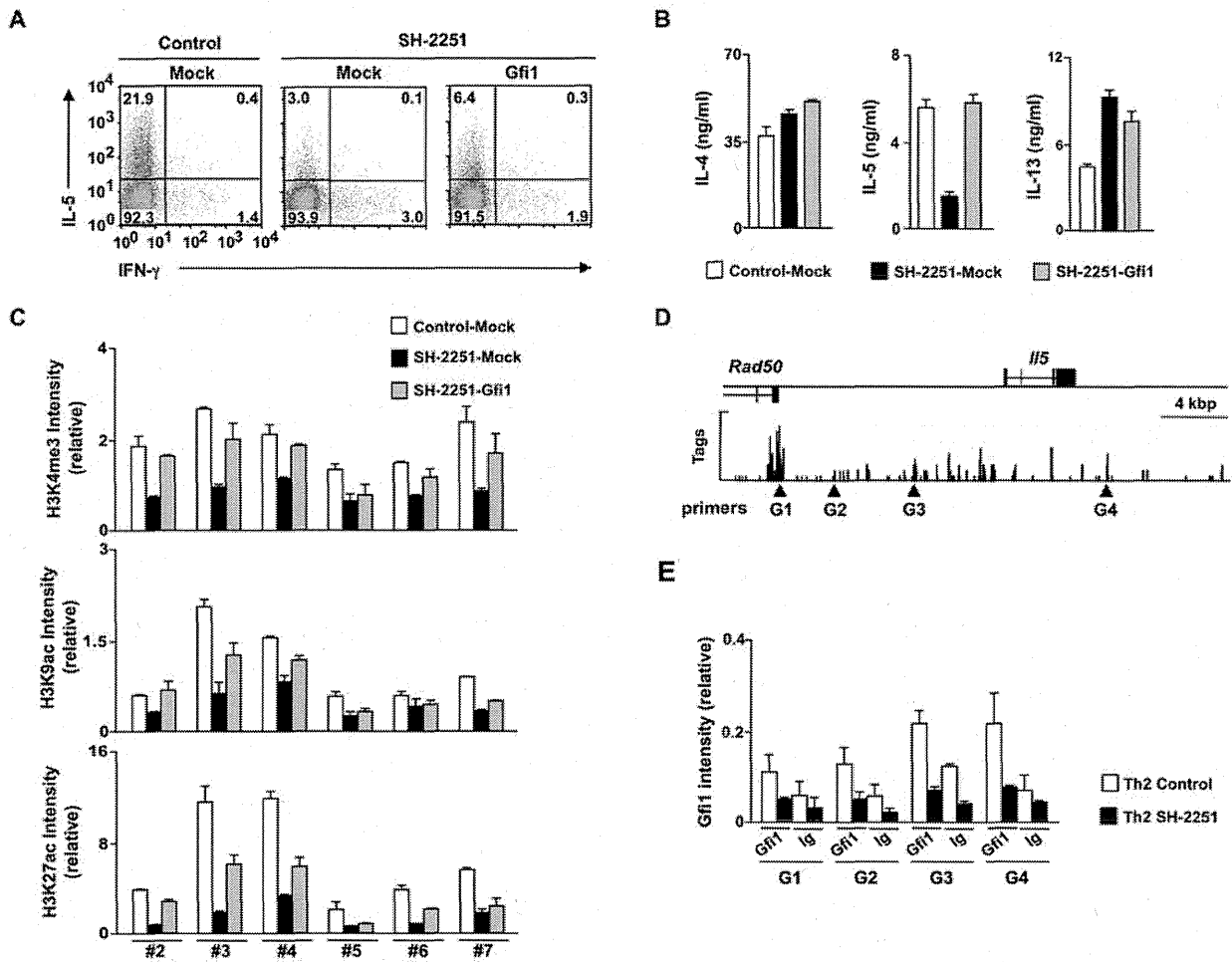


Figure 6. Transduction of *Gfi1* into SH-2251-treated Th2 cells restores the differentiation of IL-5-producing Th2 cells. (A), CD4 T cells were cultured under Th2-conditions in the presence or absence of SH-2251 (100 nM) for two days, then the cells were transduced with Mock- or *Gfi1*-IRES-hNGFR-containing retrovirus vectors. Three days after transduction, the IL-5/IFN- γ staining profiles of the transduced cells (hNGFR-positive cells) were determined with intracellular staining. The percentages of cells in each quadrant are indicated. (B), The cytokine production from SH-2251-treated Th2 cells transduced with *Gfi1* was determined. (C), Histones H3K4me3, H3K9ac and H3K27ac at the *Il5* gene locus in hNGFR-positive *Gfi1*-transduced SH-2251-treated Th2 cells. The relative intensity (/Input) is shown with the standard deviation. Three (A, B and C) independent experiments were performed with similar results. (D), The global pattern of Gfi1 binding around the *Il5* gene locus was determined using ChIP-sequencing with an anti-Gfi1 mAb. The locations of the PCR primer pairs (triangle) used in a manual ChIP assay are also listed. (E), The binding of Gfi1 around the *Il5* gene locus in SH-2251-treated Th2 cells was determined using a manual ChIP assay. The relative intensity (/Input) is shown with the standard deviation. Two independent experiments were performed with similar results. doi:10.1371/journal.pone.0061785.g006

histone, opening up the chromatin structure and increasing recruitment of RNA polymerase II [42]. Although the gene locus specific inhibitor for histone acetylation is expected to appear, such molecules have not yet been identified. We demonstrated that SH-2251 selectively inhibits induction of active histone marks, in particular H3K27ac at the *Il5* gene locus and the *Gfi1* gene locus. The transduction of *Gfi1* into SH-2251 treated Th2 cells restores the IL-5 production and active histone modifications at the *Il5* gene locus. These results indicate that SH-2251 belongs to a novel class of inhibitors that modulate histone modification status in a gene locus-specific manner.

In summary, SH-2251 selectively inhibits chromatin remodeling at the *Il5* gene locus and subsequent generation of IL-5-producing Th2 cells via attenuation of the Gfi1 expression. In addition, the oral administration of SH-2251 showed inhibitory effects on

OVA-induced airway allergic inflammation. Therefore, SH-2251 is a unique class of therapeutic candidate for allergic inflammation acting through the selective inhibition of IL-5 production.

Materials and Methods

SH-2251

SH-2251 (United States Patent No.: US 7632865 B2) was synthesized and provided by Ishihara Sangyo Kaisha, Ltd. The purity of the SH-2251 used in the experiments was 99.1%.

Mice

C57BL/6 and BALB/c mice were purchased from CLEA Japan. All mice were maintained under specific pathogen-free conditions and were used at 6–10 weeks of age. All experiments

using mice received approval from the Kazusa DNA Research Institute Administrative Panel for Animal Care. All animal care was conducted in accordance with the guidelines of the Kazusa DNA Research Institute.

CD4 T cells differentiation *in vitro*

Naïve CD4⁺ T (CD44^{lo}CD62L^{hi}) cells were prepared using a CD4⁺CD62L⁺ T cell isolation kit II (Miltenyi Biotec). Naïve CD4⁺ T cells (1.5×10^6) were stimulated with an immobilized anti-TCR- β mAb (3 μ g/ml; H57-597; BioLegend) and an anti-CD28 mAb (1 μ g/ml; 37.5; BioLegend) with or without SH-2251 (Ishihara Sangyo Kaisha, Ltd.) under the indicated culture conditions for two days. Next, the cells were transferred onto a new plate and cultured for an additional three days in the presence of cytokines with or without SH-2251. If not mentioned, 100 nM of SH-2251 was used in the experiments. The cytokine conditions for Th2 cell differentiation were as follows: IL-2 (2.5 ng/ml), IL-4 (10 ng/ml; PeproTech) and anti-IFN- γ mAb (5 μ g/ml; R4-6A2; BioLegend).

Intracellular staining of cytokines

The *in vitro* differentiated Th cells were stimulated with an immobilized anti-TCR- β mAb (3 μ g/ml; H57-597; BioLegend) for six hours in the presence of monensin (1 μ M), and intracellular staining was performed as previously described [25]. The following antibodies were used for intracellular staining: anti-IL-4-hycoerythrin (PE) mAb (11B11; BD Bioscience), IFN- γ -FITC mAb (XMG1.2; BD Bioscience), IL-5-allophycocyanin (APC) (TRFK5; eBioscience), and IL-13-PE (eBio13A; eBioscience). A flow cytometric analysis was performed using a FACSCalibur instrument (BD biosciences), and the results were analyzed using the FlowJo software program (Tree Star).

ELISA

The cells were stimulated with an immobilized anti-TCR- β mAb for 16 hours, and the culture supernatants were recovered. The amount of cytokines in the recovered supernatants was determined with ELISA, as described previously [43].

Quantitative RT-PCR

Total RNA was isolated using a TRIZOL Reagent (GIBCO). cDNA was synthesized using the Superscript VILO cDNA synthesis kit (Invitrogen). Quantitative RT-PCR was performed as previously described [43], using StepOnePlus Real-Time PCR Systems (Applied Biosystems). The specific primers, and Roche Universal Probes used in the experiments were as follows:

Hprt: 5' TCCTCCTCAGACCGCTTT 3' (forward), 5' CCTGTTTCATCATCGTAATC 3' (reverse), probe #95; *Gata3*: 5' TTATCAAGCCCCAAGCGAAG 3' (forward), TGGTGGTGGTCTGACAGTT 3' (reverse), probe #108; *Gfi1*: 5' TCCGAGTTCCGAGGACITTTG 3' (forward), 5' GAGCGGCACAGTGACTTCT 3' (reverse), probe #7.

Microarray analysis

The gene expression profiles of the SH-2251-treated Th2 cells were analyzed using the Agilent Whole Mouse 44K Array. The raw data were subjected to log₂ transformation and normalized using the Subio Platform (Subio). The gene expression data were deposited in the GSE42131.

Chromatin Immunoprecipitation (ChIP) assay and ChIP-sequencing

The Magna ChIP kit was used for the ChIP assay according to the manufacturer's protocol (MILLIPORE). The anti-histone

H3K4me2 pAb (ab7766; Abcam), anti-histone H3K4me3 pAb (cat#39159; Activemotif), anti-histone H3K27me3 pAb (cat#39155; Activemotif), anti-histone H3K36me3 pAb (ab9050; Abcam), anti-histone H3K9ac pAb (cat#39137; ActiveMotif), anti-histone H3K27ac pAb (cat#39133; ActiveMotif), anti-Gata3 (cat# AF2605; R&D) pAb and anti-Gfi1 (M-19; Santa Cruz) were used for immunoprecipitation. The specific primers at the Th2 cytokine gene locus and the Roche Universal probes used in the experiments were as follows: #1: 5' ACGCTTCCGGAAC-TAGGG 3' (forward), 5' CGCTCTGGCATCTCGTTC 3' (reverse), probe #38; #2 (G2): 5' CAGATGTGATATGCGTACATGTAATTC 3' (forward), 5' TGAACCTCT-GACCCTGCTTT 3' (reverse), probe #79; #3: 5' AGTGTCTGTCCCCGAGATCA 3' (forward), 5' GCTGCCTGGAACCTTGGTG 3' (reverse), probe #64; #4: (Il5p), 5' TCACCTTATCAGGAATTGAGTTTAAACA 3' (forward), 5' GATCGGCCTTTTCTTGGCA 3' (reverse), probe #43; #5: 5' TGCCCTCTCTTTTGTTTTCCCTTG 3' (forward), 5' GCAATTCAGTGGTAGAGT

GCTCA 3' (reverse), probe #81; #6 (G4): 5' AGTACAAGGGCCAAGTCACG 3' (forward), 5' GCCAGACACTGGGGTAAAGT 3' (reverse), probe #16; #7: 5' GCTGGCCTTGAACCTTACTACG 3' (forward), 5' GTGTGTACCCGTAATCCCA

AC 3' (reverse), probe #10; G1: 5' GGAAGTGGGAGTCC-TAAGCA 3' (forward), 5' CTCCCTGCCCAACTTCTAAA 3' (reverse), probe #15; G3: 5' AAGGGGAGAAGTGCCTCTCTA 3' (forward), 5' TCATGCCATGGGATACAGG (reverse), probe #99; Il4p: 5' TTGGTCTGATTTTACAGGAAAA 3' (forward), 5' GGCCAATCAGCACCTCTCT 3' (reverse), probe #2; V_A site in the IL-4 enhancer: 5' GCCTGTTTCCCTCTCAGCATT 3' (forward), 5' TGATAAAAGTGACTTGAAGGTT

GG 3' (reverse), probe #4; IL-4 intronic enhancer: 5' CCCAAAGGAGGTGCTTTT

ATC 3' (forward), 5' AAATCCGAAACTGAGGAGTGC 3' (reverse), probe #75; Il13p: 5' CCAGGTTCTGGGTGGTT-TATT 3' (forward), 5' GAATTACTGGGGCGGAAGTT 3' (reverse), probe #105; Rad50p: 5' GGAAGTGGGAGTCC-TAAGCA 3' (forward), 5' CTCCCTGCCCAACTTCTAAA 3' (reverse), probe #15. The specific primers at the Gfi1 gene locus and the Roche Universal probes used in the experiments were as follows:

a: 5' TTTGCAGAAGAGTGAGGTTTGA 3' (forward), 5' TGGAGGCGTGGGATTAAC 3' (reverse), probe #55; b: 5' GACCAAGGCGTGTGA

CTATACA 3' (forward), 5' CACACCCTGTTGTACC-CACTT 3' (reverse), probe #48; c: 5' GTGCCACACCAC-TATTCCAG 3' (forward), 5' AGTGGCAAAGGACCAAC

ACT 3' (reverse), probe #2; d: 5' TGGGGACAGGTTT-TACCACT 3' (forward), 5' GACAGGTGGCAGCAATCC 3' (reverse), probe #70.

The samples for the ChIP-sequencing were prepared according to the manufacturer's protocol (Illumina), and the ChIP-sequencing was performed using Genome Analyzer Ix (Illumina).

Immunoblot analysis

Cytoplasmic and nuclear extracts were prepared using NE-PER Nuclear and Cytoplasmic Extraction Regents (Thermo Fisher Scientific) as previously described [43]. Anti-Gata3 mAb (HG3-31; Santa Cruz), anti-Gfi1 pAb (M-19; Santa Cruz) and anti- α -Tubulin mAb (DM1A; Lab Vision) were used for the immunoblot analysis.

Retrovirus-mediated gene transfer

The methods for generating retrovirus supernatant and infection were described previously [25]. Infected cells were detected using staining with anti-human NGFR-PE mAb (ME20.4-1.H4; Miltenyi Biotec) and anti-PE microbeads (#130-048-801; Miltenyi Biotec), and hNGFR-positive infected cells were purified using AutoMACS (Miltenyi Biotec).

Luciferase assay

The IL-5 promoter activity was determined as previously described [30]. In brief, M12 cells (B cell line) were cotransfected with a firefly luciferase reporter (pGL3-*IL5* promoter), a renilla luciferase plasmid (pRL-TK; Promega) and an expression vector (pFlag-CMV2; Sigma) using Gene Pulser MXcell (BIO-RAD). Twenty-four hours after transfection, the cells were maintained in the presence or absence of SH-2251 for one hour, and then stimulated with PMA plus dibuteryl-cAMP for 12 hours. The luciferase activity was measured using a Dual-Luciferase Reporter Assay System (Promega).

OVA-induced allergic airway inflammation

BALB/c mice were immunized intraperitoneally with 100 μ g OVA in 2 mg of aluminum hydroxide gel on day 0. Next, the mice were intranasally challenged with OVA in saline (100 μ g/mouse) on days 8 and 10. SH-2251 (10 mg/kg) was orally administered every day from day 0 to day 11. Two days after the last OVA challenge, BAL fluid cells and lung samples were prepared for histological examination as previously described [44]. Lung mononuclear cells were also prepared two days after the last OVA challenge, as previously described [45]. CD4 T cells were purified from lung mononuclear cells using anti-mouse CD4 microbeads (Miltenyi Biotec).

Statistical analysis

Student's *t*-test was used for the statistical analyses. ANOVA and the Bonferroni-test were used in the *in vivo* experiments.

References

- Adcock IM, Caramori G, Chung KF (2008) New targets for drug development in asthma. *Lancet* 372: 1073–1087.
- Holgate ST (2008) Pathogenesis of asthma. *Clin Exp Allergy* 38: 872–897.
- Bosnjak B, Sreelzmueller B, Erb KJ, Epstein MM (2011) Treatment of allergic asthma: modulation of Th2 cells and their responses. *Respir Res* 12: 114.
- Kouro T, Takatsu K (2009) IL-5- and eosinophil-mediated inflammation: from discovery to therapy. *Int Immunol* 21: 1303–1309.
- Rothenberg ME, Hogan SP (2006) The eosinophil. *Annu Rev Immunol* 24: 147–174.
- Gauvreau GM, Ellis AK, Denburg JA (2009) Haemopoietic processes in allergic disease: eosinophil/basophil development. *Clin Exp Allergy* 39: 1297–1306.
- Foster PS, Hogan SP, Ramsay AJ, Matthaci KI, Young IG (1996) Interleukin 5 deficiency abolishes eosinophilia, airways hyperreactivity, and lung damage in a mouse asthma model. *J Exp Med* 183: 195–201.
- Wei L, Vahedi G, Sun HW, Watford WT, Takatori H, et al. (2010) Discrete roles of STAT4 and STAT6 transcription factors in tuning epigenetic modifications and transcription during T helper cell differentiation. *Immunity* 32: 840–851.
- Ansel KM, Djuretic I, Tanasa B, Rao A (2006) Regulation of Th2 differentiation and Il4 locus accessibility. *Annu Rev Immunol* 24: 607–656.
- Wilson CB, Rowell E, Sekimata M (2009) Epigenetic control of T-helper-cell differentiation. *Nat Rev Immunol* 9: 91–105.
- Nakayama T, Yamashita M (2008) Initiation and maintenance of Th2 cell identity. *Curr Opin Immunol* 20: 265–271.
- Zhu J, Yamane H, Paul WE (2010) Differentiation of effector CD4 T cell populations (*). *Annu Rev Immunol* 28: 445–489.
- Taniguchi M, Tashiro T, Dashisoodol N, Hongo N, Watarai H (2010) The specialized iNKT cell system recognizes glycolipid antigens and bridges the innate and acquired immune systems with potential applications for cancer therapy. *Int Immunol* 22: 1–6.

Supporting Information

File S1 The effects of SH-2251 on Th1-, Th9-, and Th17-differentiation. Naive CD4 T cells were cultured under Th1- (A), Th9- (B) or Th17- (C) conditions in the presence or absence of SH-2251 (100 nM) for five days. The cells were restimulated with an immobilized anti-TCR- β mAb for six hours, and the intracellular staining profiles were determined using intracellular staining (left). The following antibodies were used for intracellular staining: anti-IL-4-PE mAb (11B11; BD Bioscience), IFN- γ -FITC mAb (XMG1.2; BD Bioscience), anti-IL-9-PE mAb (RM9A4; BioLegend), anti-IL-17A-Alexa647 mAb (TC11-18H10.1; BioLegend) and IL-17F-Alexa488 mAb (9D3.1C8; BioLegend). The percentages of each quadrant are indicated. The cytokine production by the SH-2251-treated Th cells stimulated with an immobilized anti-TCR- β mAb for 16 hours was determined with ELISA. The culture conditions for each Th cell differentiations were as follows. Th1-conditions: IL-2 (2.5 ng/ml), IL-12 (1 ng/ml; PeproTech) and anti-IL-4 mAb (5 μ g/ml; 11B11; BioLegend). Th9-conditions: IL-2 (2.5 ng/ml), IL-4 (10 ng/ml), TGF- β (10 ng/ml; PeproTech) and anti-IFN- γ mAb (5 μ g/ml). The Th17-conditions were as follows: IL-6 (10 ng/ml; PeproTech), IL-1 β (5 ng/ml; PeproTech), TGF- β (1 ng/ml), anti-IL-2 (5 μ g/ml; BioLegend), anti-IL-4 mAb (5 μ g/ml) and anti-IFN- γ mAb. Three independent experiments were performed with similar results. **P*<0.05 and ***P*<0.01 (Student's *t*-test). (DOCX)

Acknowledgments

We thank, Mr. Takashi Watanabe, Mr. Kazuhiro Sato, Mr. Masaki Takazawa, Ms. Yasuyo Tanaka and Ms. Noriko Nakashio for their excellent technical assistance.

Author Contributions

Conceived and designed the experiments: JS MY. Performed the experiments: JS MK ST TN OO MY. Analyzed the data: JS MK. Contributed reagents/materials/analysis tools: MI FK. Wrote the paper: JS MY.